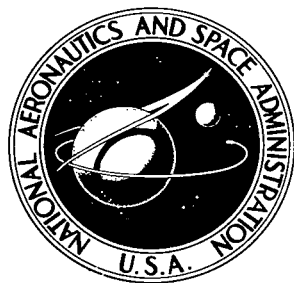
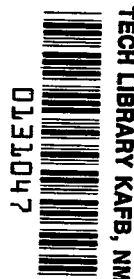


NASA TECHNICAL NOTE



NASA TN D-4596

C. 1



NASA TN D-4596

LOAN COPY: RETURN TO  
AFWL (WLIL-2)  
KIRTLAND AFB, N MEX

# THE FABRICATION AND TESTING OF PAGEOS I

*by Louis A. Teichman*  
*Langley Research Center*  
*Langley Station, Hampton, Va.*





0131047

NASA TN D-4596

THE FABRICATION AND TESTING OF PAGEOS I

By Louis A. Teichman

Langley Research Center  
Langley Station, Hampton, Va.

NATIONAL AERONAUTICS AND SPACE ADMINISTRATION

---

For sale by the Clearinghouse for Federal Scientific and Technical Information  
Springfield, Virginia 22151 - CFSTI price \$3.00

# THE FABRICATION AND TESTING OF PAGEOS I

By Louis A. Teichman  
Langley Research Center

## SUMMARY

As an aid in assuring the successful construction and deployment of PAGEOS I, detailed fabrication process specifications were prepared and an extensive testing program was conducted. This large body of information on fabrication processes, testing techniques, and material properties is summarized herein as an indication of the present state of the art of inflatable sphere technology.

## INTRODUCTION

PAGEOS I (an acronym for PAssive Geodetic Earth Orbiting Satellite), shown in figure 1, is a 100-foot-diameter (30.48 meter) sphere, constructed of 0.5-mil-thick ( $1.27 \times 10^{-2}$  mm) poly(ethylene terephthalate) film (hereinafter called PET), and coated on its exterior with vapor-deposited aluminum to make it highly reflective of sunlight. It was erected in space to spherical shape from a compactly folded condition within a canister after being placed into a near-polar and circular orbit of 2288 nautical miles (4237 kilometers) altitude on June 24, 1966. Its launching was a part of the NASA effort in support of the National Geodetic Satellite Program (ref. 1). The basic function of PAGEOS I is to provide a luminous target in near-earth space that can be simultaneously photographed against a star background from two or more widely separated ground stations of a worldwide geodetic network (fig. 2). The photographs will provide measurements of the shape and size of the earth, and location of points on the earth relative to each other, by geometric means which are independent of the earth's gravitational field.

PAGEOS I is a technologically advanced version of the Echo I passive communications research satellite (ref. 2). In addition to its use for communications research, Echo I has served as a test satellite for the development of the method of satellite triangulation (refs. 3, 4, and 5) and as a long-duration test of the satellite structure and materials in the space environment (ref. 6).

A computer program, modified to reflect the changes in the orbit of Echo I under the influence of solar radiation pressure, was used to select a stable PAGEOS orbit (ref. 7) which would provide a geodetically useful lifetime of at least 5 years and which would insure adequate coverage of all ground stations (ref. 8). The orbit of Echo I has

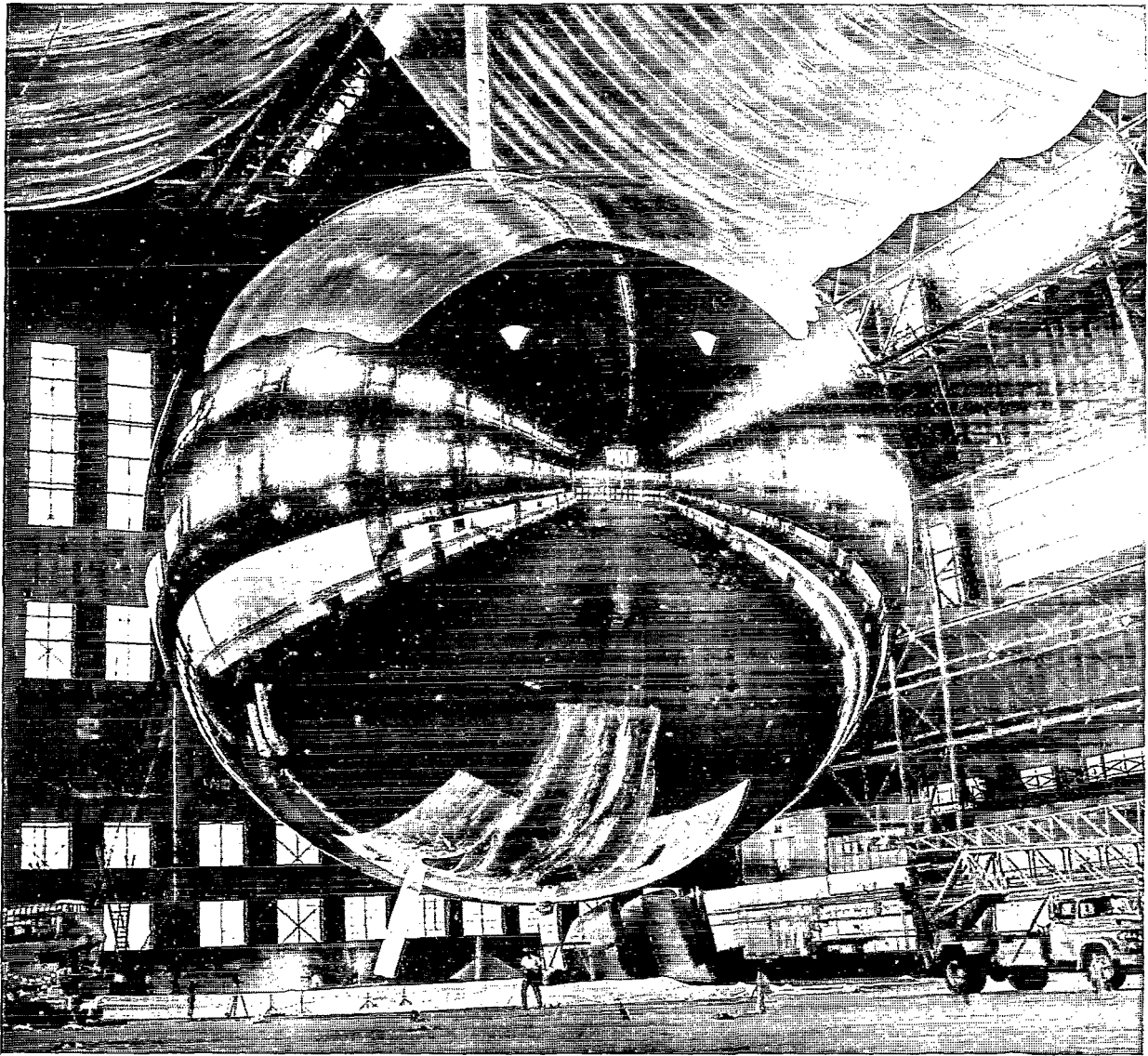


Figure 1- The fully inflated PAGEOS I static inflation test prototype.

65-H-1339

too low an inclination and altitude to permit its use for establishing a worldwide geodetic network (which requires the spanning of intercontinental distances) but is geodetically useful for local network densification.

PAGEOS I and the earlier Echo I represent satellites of a unique design and hence include a large body of technology not common with other spacecraft. The purpose of this report is to set forth the state of this technology at the time of the successful launching of PAGEOS I. The scope of the technology presented thus embraces all the relevant earlier technology of Echo I as well as the extensive revisions, extensions, and additions thereto accomplished in designing, constructing, testing, and launching PAGEOS I.

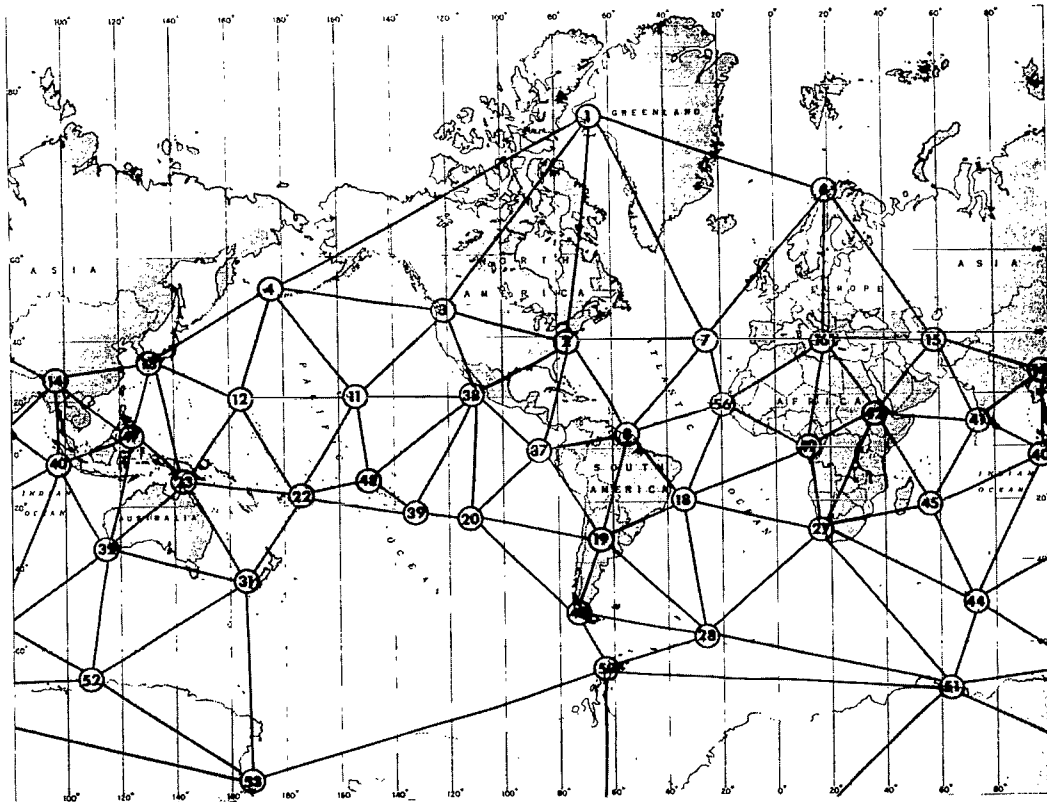


Figure 2.- Primary PAGEOS network.

### SYMBOLS

- a earth's albedo, 0.36
- $C_S$  solar radiation constant,  $1.3953 \times 10^3$  watt/meter<sup>2</sup>
- c velocity of light in vacuo,  $2.99776 \times 10^{10}$  cm-sec<sup>-1</sup>
- D satellite diameter, feet (meter)
- E modulus of elasticity of PET,  $3.8 \times 10^5$  newton-cm<sup>-2</sup>
- $F_R(\beta)$  ratio of earth-reflected energy incident on satellite relative to amount incident when angular displacement  $\beta$  between earth-satellite and earth-sun lines is zero

|                           |  |
|---------------------------|--|
| f                         | PAGEOS I air orifice hole area, 3.325 cm <sup>2</sup>  |
| g                         | PAGEOS I micrometeoroid hole growth rate, 3.25 × 10 <sup>-4</sup> cm <sup>2</sup> -sec <sup>-1</sup> |
| h                         | satellite altitude, feet (meters)  |
| $k = \frac{R_E}{R_E + h}$ |  |
| M                         | molecular weight   |
| m                         | satellite mass, pounds (kilograms)   |
| p                         | pressure, pounds force/inch <sup>2</sup> (newtons/meter <sup>2</sup> )                               |
| P                         | probability  |
| R                         | radius, feet (meters)  |
| R <sub>g</sub>            | universal gas constant, 8.314 joule-mole <sup>-1</sup> -°K <sup>-1</sup>                             |
| T                         | absolute temperature, °K   |
| t                         | time, sec  |
| t'                        | thickness of PAGEOS I material, 1.27 × 10 <sup>-3</sup> cm   |
| V                         | satellite volume, cubic feet (meter <sup>3</sup> )   |
| x,y                       | distances along X- and Y-axes, feet (meters)   |
| α                         | total absorptance of PAGEOS aluminum-coated PET to thermal radiation, 0.10                           |
| W                         | weight of inflation compound, pound mass (kilograms)   |
| ε <sub>o</sub>            | total hemispherical emittance of the outside surface of PAGEOS I, 0.03                               |
| ε <sub>i</sub>            | total hemispherical emittance of the inside surface of PAGEOS I, 0.45                                |

|          |   |
|----------|---|
| $\nu$    | Poisson's ratio for PET, 0.5  |
| $\sigma$ | Stefan-Boltzmann radiation constant, $5.70 \times 10^{-8} \text{ watt-m}^{-2}\text{-}^{\circ}\text{K}^{-4}$ |

Subscripts:

|    |                         |
|----|-------------------------|
| a  | anthraquinone           |
| b  | satellite; benzoic acid |
| C  | coldspot; curvature     |
| cr | critical                |
| E  | earth                   |
| H  | hotspot                 |
| o  | initial                 |
| s  | solar                   |
| sh | shadow                  |
| su | sunlight                |

Bars over symbols indicate average values.

### PAGEOS I MISSION

The mission of PAGEOS I is to provide a luminous target in near-earth space that fulfills the requirements for worldwide satellite triangulation, as described below:

If a satellite in sunlight reflects sufficient light to ground observation stations located in darkness, such as A, B, and C in figure 3, the satellite can be photographed from the stations as a point of light against a background of stars. Simultaneous photographs of the satellite from two ground stations, such as A and B, provide, from the known positions of the background stars on the celestial sphere, the directions in space of the lines from the two stations to the satellite. These two lines define a plane that includes the base line AB between the stations, even though the stations are not visible

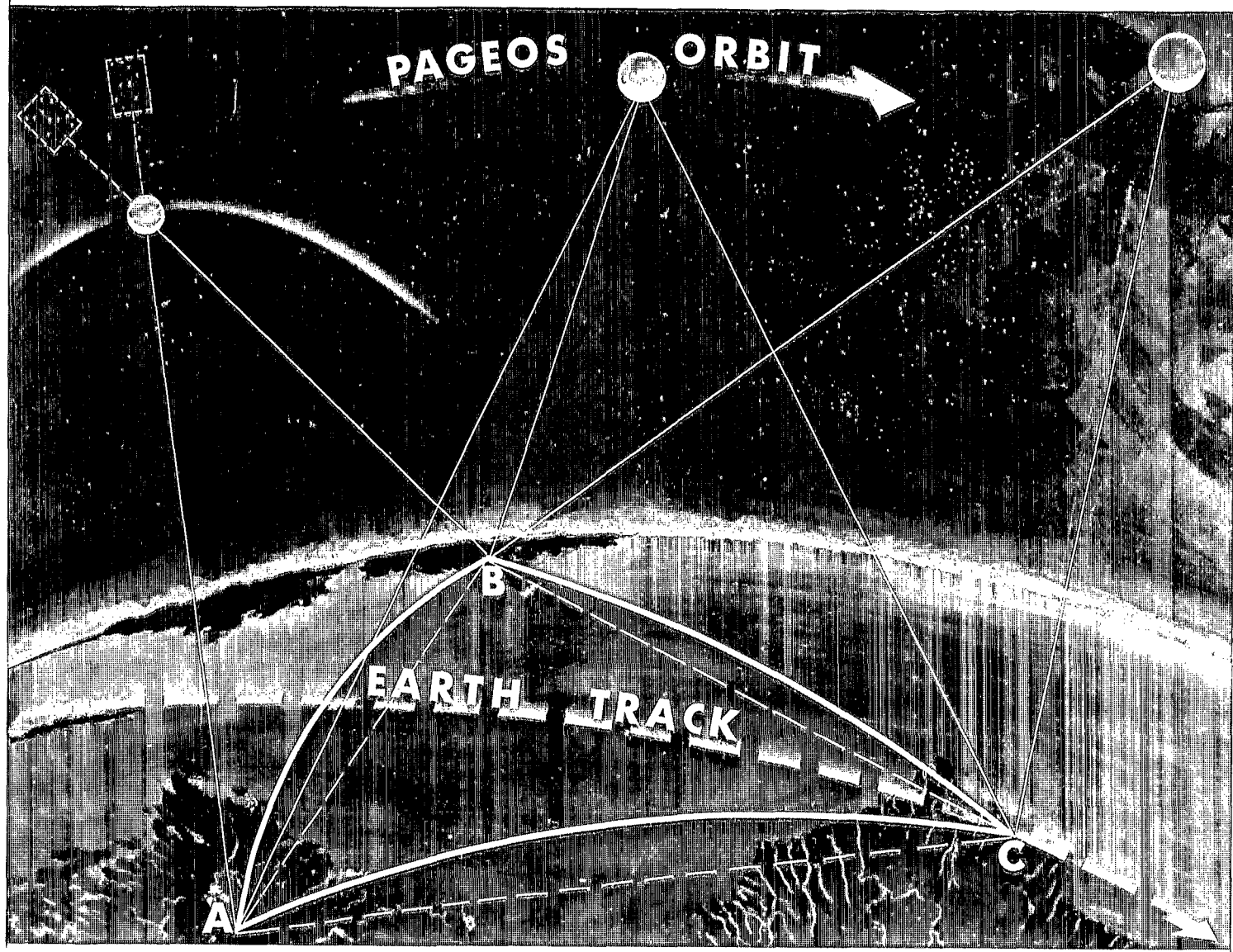


Figure 3.- Simultaneous observations of PAGEOS against star background.



to each other. A second pair of simultaneous photographs from stations A and B taken with the satellite in a different position, preferably at a displacement greater than  $60^{\circ}$  about the base line AB, similarly defines a second plane that also includes the base line AB. Because the first and second planes are not defined at the same instant of time, one must be rotated in space about the earth's axis relative to the other to correct for the time difference, a correction which is readily made since the earth's rate of rotation is accurately known. At the common instant of time to which the planes are corrected, the planes define the direction in space, relative to the celestial sphere, of the base line AB. Continuation of this procedure between all adjacent stations in a worldwide network of stations, such as that shown in figure 2, yields, for a common instant of time, the spatial direction of each base line connecting the stations, and hence the shape of the network of base lines.

The size of the network is determined by measurement of the length of at least one base line by conventional means. The size and shape of the network is thereby established by purely geometric means with no dependence on the gravitational field of the earth. Since the position of the stations in the worldwide network can then be located by conventional means relative to their local geodetic surveys, the local geodetic surveys are thereby interconnected through the worldwide network.

This method of triangulation described requires that the satellite continuously reflect sunlight to each of the ground stations that are simultaneously photographing it. The condition is satisfied by the highly specular surface of PAGEOS I. However, since the position of the sun's image on the satellite is a function of the camera-satellite-sun angle (phase angle), the direction of the satellite must be corrected to a common point in space to yield geodetically consistent results. A spherical satellite permits accurate corrections by referencing all directions to the center of the sphere.

The requirement for an initial nominal altitude of approximately 2295 nautical miles (4250 kilometers) and an inclination of  $87^{\circ}$  prograde was dictated by considerations of geodetic network geometry (ref. 8) and orbit stability. For this orbit and its expected perturbations during a 5-year lifetime, it was found that an Echo I type of satellite satisfied the brightness, sphericity, and specularity requirements of the geodetic mission.

The required size of PAGEOS I necessitated its launch in a folded configuration. This configuration in turn required that launch-vehicle—spacecraft separation and canister-half separation be accomplished in a manner which would preclude interference with successful inflation. Thus, the 100-foot-diameter (30.48 meter) inflatable sphere was folded into a magnesium canister (ref. 9) which was in turn adapted to the thrust face of an Agena-D second-stage vehicle by a truncated aluminum cone (fig. 4). The Agena-D vehicle (fig. 5) was mounted on top of a thrust-augmented Thor first stage

(fig. 6). After the Agena achieved orbit, the canister was ejected from the adapter by a single-spring mechanism at a differential velocity of about 6 feet per second (1.8 m/sec). After a programmed delay of 83.5 seconds, the canister halves were separated by the impact force of a shaped charge at a relative velocity of about 50 feet per second (15.2 m/sec); thus, the satellite was left to be inflated about 500 feet (152.4 meters) ahead of the vehicle.

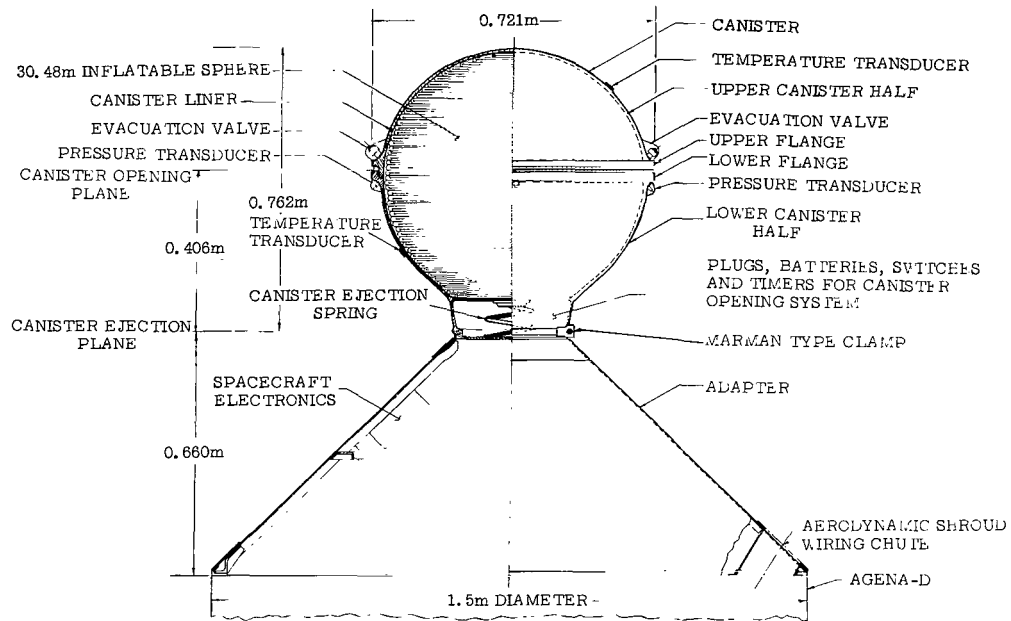


Figure 4.- PAGEOS I spacecraft assembly.

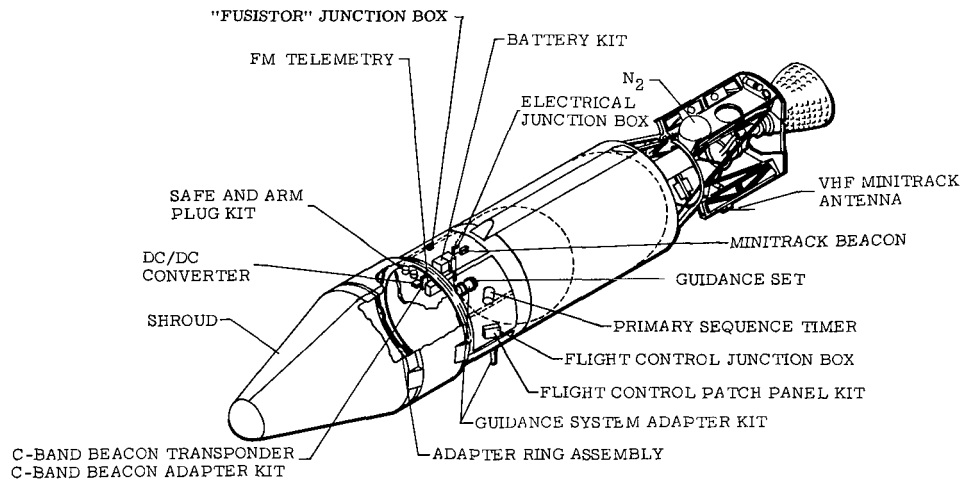


Figure 5.- Agena subassemblies peculiar to PAGEOS I mission.

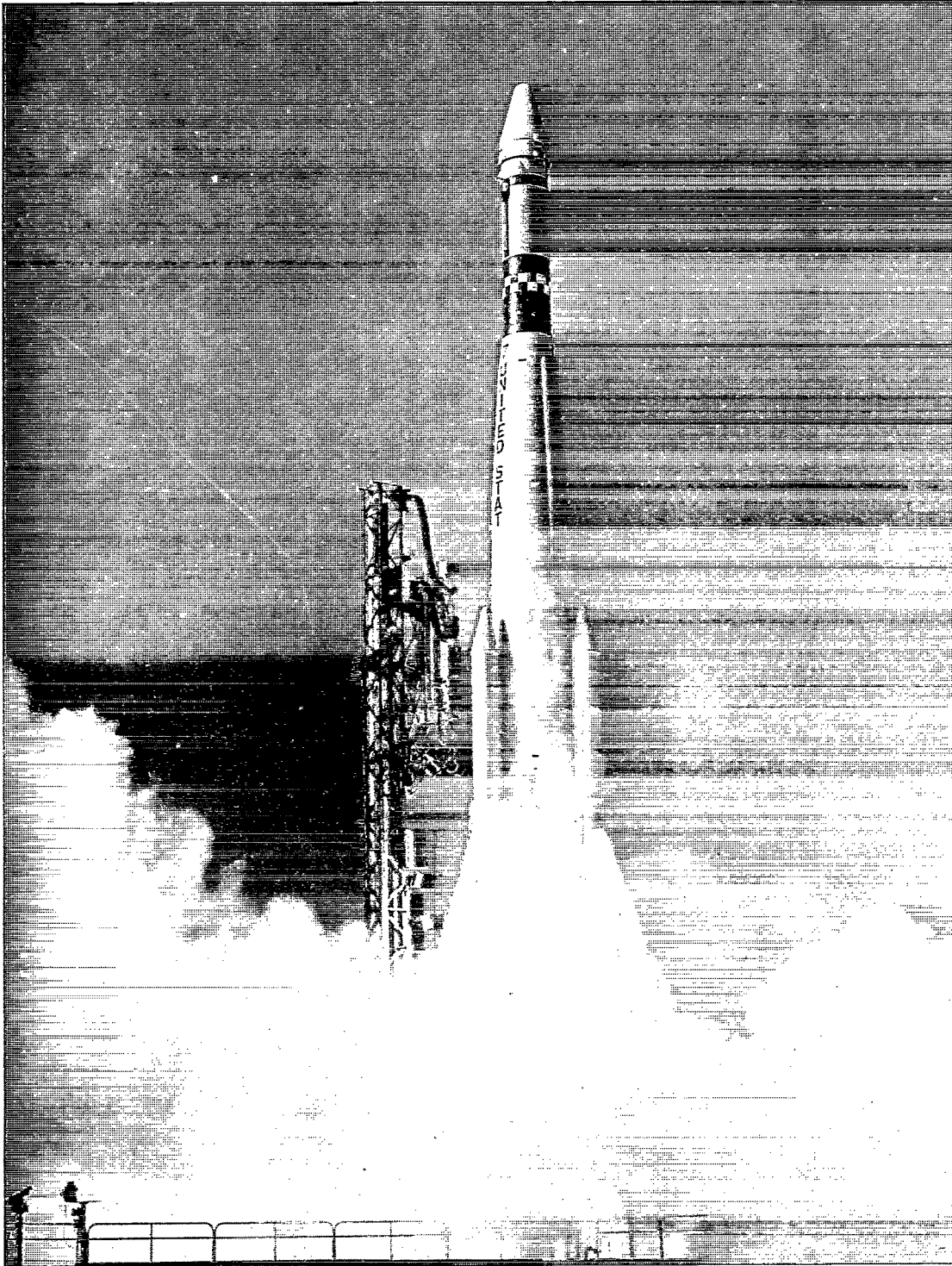


Figure 6.- PAGEOS I launch vehicle.

L-66-6023

## INFLATABLE SPHERE FABRICATION

In order to qualify PAGEOS I for its mission, two prototype inflatable spheres were fabricated. The first prototype was built for the purpose of conducting a static inflation test as a means of confirming the structural integrity of the sphere. The second prototype was employed in the conduct of a full-scale deployment test. A third sphere was fabricated for actual flight. Three additional inflatable spheres were fabricated for backups and spares.

The testing of the two prototype spheres revealed errors in spacecraft design and fabrication and led to corrective measures which were applied in the production of the flight article. The following discussion is therefore limited to the fabrication of the successful flight sphere; the discussion of the errors revealed by fabrication and testing of the prototypes and the corrective measures instituted to overcome them are reserved for later sections of this report.

### Chemical Treatment

The PAGEOS I inflatable sphere was fabricated (ref. 10) of 0.5-mil ( $1.27 \times 10^{-2}$  m) PET film coated on the outside surface with approximately 2000 angstroms of vapor-deposited aluminum. Upon receipt of the PAGEOS I material in roll form, the plastic side of the film was chemically treated with a cleaning solution consisting of 53 parts per million (ppm) of a cationic detergent in freon. The chemical treatment process, depicted schematically in figure 7, was employed to prevent plastic-to-plastic adhesion of the sphere during its fabrication and in its packaged flight configuration; this condition could have caused tearing during inflation of the sphere in space.

Empirically determined specifications for maximum effectiveness in chemical treatment were as follows:

- (1) Material roll speed,  $12 \pm 2$  feet per minute ( $6.1 \pm 1 \times 10^{-2}$  m/sec)
- (2) Material roll tension, minimum
- (3) Reverse roller speed,  $20 \pm 2$  revolutions per minute
- (4) Treatment solution inflow rate, 500 milliliters per minute  
( $5 \times 10^{-4}$  m<sup>3</sup>/min or  $8.3 \times 10^{-6}$  m<sup>3</sup>/sec)
- (5) Treatment solution drainage rate, 200 to 400 millimeters ( $2$  to  $4 \times 10^{-4}$  m<sup>3</sup>)  
per minute (evaporation and material coating accounts for the inflow-outflow difference)
- (6) Treatment solution temperature,  $70^{\circ} \pm 10^{\circ}$  F ( $21^{\circ} \pm 5.6^{\circ}$  C)
- (7) First drying tunnel temperature, room temperature
- (8) Second drying tunnel temperature,  $130^{\circ} \pm 10^{\circ}$  F ( $54.4^{\circ} \pm 5.6^{\circ}$  C)

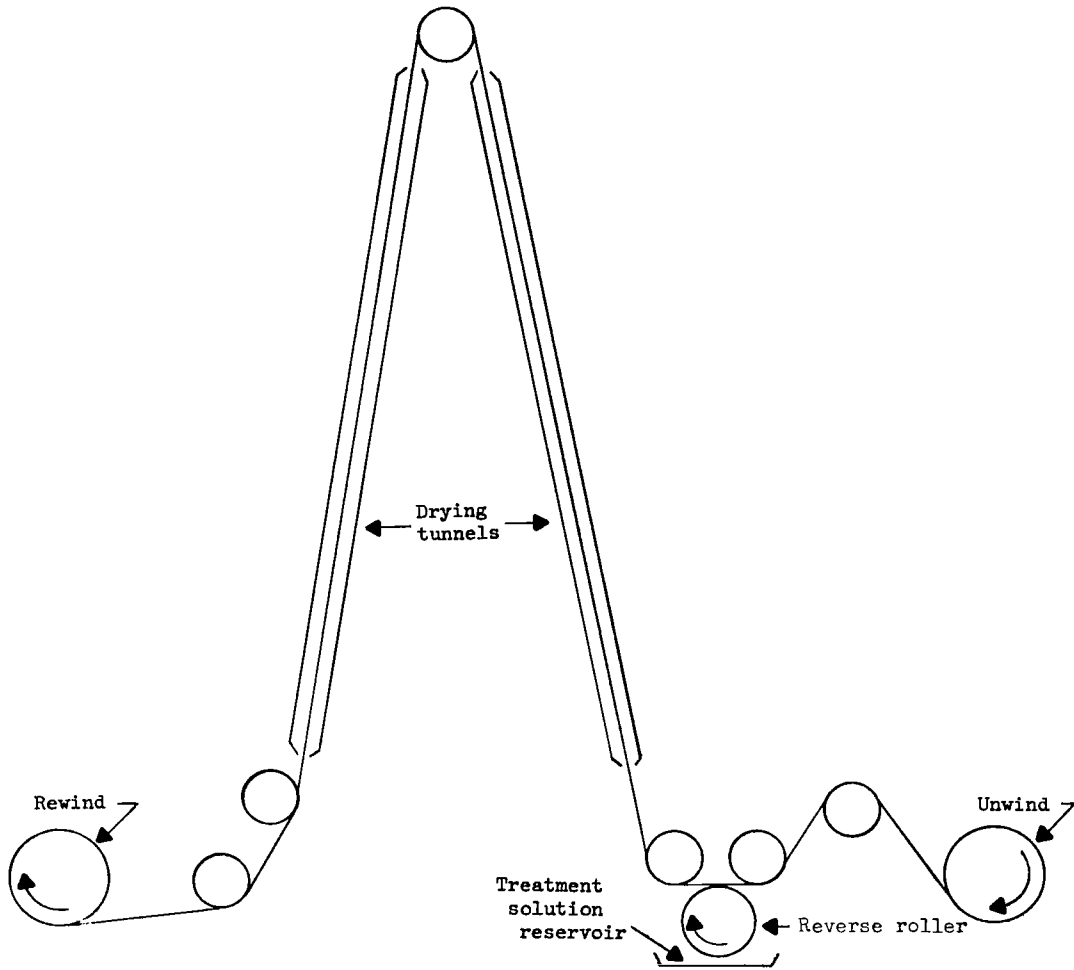


Figure 7.- Schematic of chemical treatment apparatus.

## Visual Inspection

Visual inspection of the PAGEOS I material for defects was divided into two parts. Gross checks for cuts, burns, tears, processing marks, large holes, and metalizing voids were conducted at all stages of inflatable-sphere fabrication. Additional inspection for small holes and metalizing voids was conducted, immediately after chemical treatment, in a darkened cubicle in which the metalized side of the material was illuminated with 100 foot candles ( $1.08 \times 10^3$  lumens/meter<sup>2</sup>) of light located 2 inches (50.8 mm) away from the roll. Metalizing voids whose maximum dimension was greater than 0.020 inch (0.508 mm) and less than 0.125 inch (3.18 mm) were patched on the aluminized side of the PAGEOS I material at the gore cutting table. Material with metalizing voids less than 0.020 inch was accepted without patching and material with voids greater than 0.125 inch was rejected. Holes in the PAGEOS I material whose maximum dimension was greater than 0.020 inch and less than 0.063 inch (1.60 mm) were patched on the PET side. Material with holes less than 0.020 inch was accepted, whereas material with holes greater than 0.063 inch was rejected. In addition, a maximum of four patched holes were permitted per gore blank before assembly. Material with a hole which would be closer to a prospective gore edge than 2 inches was rejected. All patches were made of PAGEOS I material on which a thermosetting heat-sealable adhesive had been applied to the PET side. A hand-held sealing iron was employed in application of the patches. The tolerances for acceptable, patched, and rejected metalizing voids and holes were determined empirically. Numerous tests verified that material with acceptable holes and voids, as defined above, would in no way compromise the PAGEOS mission.

## Gore Cutting, Weighing, and Sealing

To form an inflatable sphere, 84 ellipsoidal gores, each 157 feet long (47.85 m) and 45 inches (1.14 m) in maximum width (see table I for accurate length-width configuration) were taped together on the inside surface with a 1-inch-wide (25.4 mm) splice plate tape (made from the same material as the gores) so that a plastic-adhesive-plastic bond was formed (fig. 8). The tape was coated with a proprietary thermosetting heat-sealable adhesive on the PET side of the basic fabrication material.

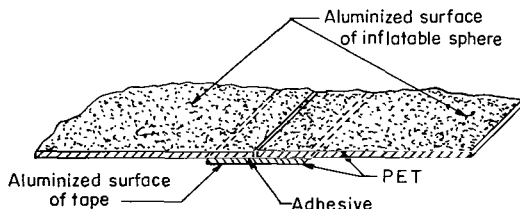


Figure 8.- PAGEOS gore seam.

Each gore was individually cut on a 160-foot-long (48.77 m) 51-inch-wide (1.30 m) table fitted with a template which formed the outline of the gore. The template had the correct contour in width to within  $\pm 0.030$  inch (0.762 mm) 30 feet (9.14 m) each side of the

TABLE I.- GORE CONFIGURATION

| Distance from equator |        | Gore width     |               |
|-----------------------|--------|----------------|---------------|
| feet                  | meters | inch           | millimeter    |
| 0                     | 0      | 44.880 ± 0.030 | 1140.0 ± 0.76 |
| 8.734                 | 2.662  | 44.198 ± .030  | 1122.6 ± .76  |
| 17.468                | 5.324  | 42.174 ± .030  | 1071.2 ± .76  |
| 26.202                | 7.986  | 38.868 ± .030  | 987.25 ± .76  |
| 34.936                | 10.648 | 34.380 ± .020  | 873.25 ± .51  |
| 42.797                | 13.045 | 29.444 ± .020  | 747.88 ± .51  |
| 52.404                | 15.973 | 22.440 ± .020  | 569.98 ± .51  |
| 61.404                | 18.716 | 15.350 ± .015  | 389.89 ± .38  |
| 65.505                | 19.966 | 11.616 ± .015  | 295.05 ± .38  |
| 69.872                | 21.297 | 7.794 ± .015   | 198.0 ± .38   |
| 74.239                | 22.628 | 3.912 ± .015   | 99.36 ± .38   |
| 78.606                | 23.959 | 0              | 0             |

equator (the plane of maximum width); within ±0.020 inch (0.508 mm) from 30 to 60 feet (9.14 to 18.3 m) each side of the equator; and within ±0.015 inch (0.381 mm) from 60 feet each side of the equator to the tip end of the template. In addition, the template was designed to be accurate to ±0.25 inch (6.35 mm) in length and its center line was designed to be straight to within 0.062 inch (1.57 mm). (Actual maximum deviations measured were 0.096 inch (2.44 mm) in length and 0.046 inch (1.17 mm) in straightness.) Five randomly selected stations of the gore-cutting template were checked for accuracy of width at least twice every 8-hour shift. In addition, the entire template was checked prior to gore cutting for each new sphere.

After cutting, the gores were weighed and stored in a roll prior to sealing. The required gore mass was 627 ± 64 grams. In addition, gore positions were determined by weight. Gores whose masses were equal to within 13.6 grams were positioned in the sphere 90° apart for balancing. The total inflatable sphere mass, including gores, tapes, repairs, and polar caps, but excluding the inflation system, was required to be 130 pounds (59.02 kg) or less. In actual practice, all gores weighed between 586 and 640 grams and were matched by quadrants to within 12 grams. PAGEOS I weighed 119.2 pounds (54.12 kg).

Seam tapes were applied with a motor-driven sealing machine. The maximum gap permitted between gores was 0.030 inch (0.762 mm), except within 5 feet (1.52 m) of each polar cap, where the maximum permissible gap was 0.020 inch (0.508 mm). The maximum overlap permitted was 0.040 inch (1.02 mm), except within 5 feet of each polar

cap where only a 0.020-inch overlap was allowed. These tolerances were not exceeded on the flight sphere.

Failure to meet the sealing specifications given, or the seal test specifications described in a later section, necessitated the application of aluminized PET repair tapes, and in certain more serious cases, removal of the gore from the inflatable sphere. Repair of out-of-specification seams which did not require cutting of the butt joint was performed by the application of a 3/4-inch-wide (19.1 mm) tape to the outside surface of the inflatable sphere. When seam repairs required cutting of the butt joint, an additional 2-inch-wide (50.8 mm) tape was applied to the inside surface. Limitations were placed on the permissible individual and total lengths of repairs (8 feet (2.44 m) and 15 feet (4.57 m) per seal, respectively). Gore removal proved unnecessary on the flight sphere. If a gore had been removed, procedures called for the use of a 1.5-inch-wide (38.10 mm) tape in the inside surface of the balloon and a 3/4-inch-wide tape on the outside surface. The final seal of each inflatable sphere was made by application of a 3/4-inch-wide tape to the inside surface and a 1-inch-wide (25.4 mm) tape to the outside surface.

To facilitate residual air evacuation during the packaging operation, two gores, 180° apart, of each inflatable sphere were vented with 84 reinforced vent holes (fig. 9). These vent holes were distributed evenly along a line which circumscribes the sphere. The gores were pleat folded so that the holes were located in the center of the outside gores and then accordion folded so that the final locations of the holes were on the inside and outside of each fold when installed in the canister.

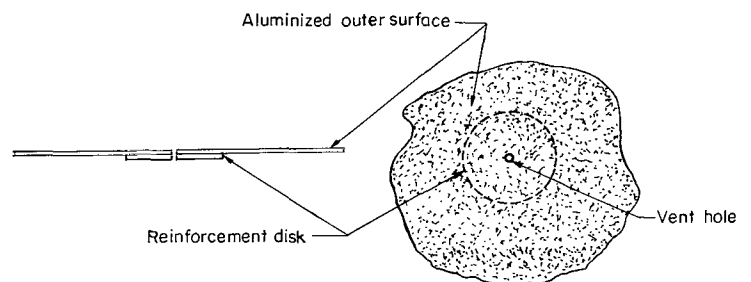


Figure 9.- PAGEOS vent hole configuration

### Polar Cap Configuration

The ends of the gores were terminated on the inner of two polar caps. (See fig. 10.) The inner polar cap, designed to be the load-carrying member, was cut from 1.0-mil-thick ( $1.27 \times 10^{-2}$  mm) PET, 38 inches (0.965 m) in diameter, and was bonded to the gore ends with a 2-inch-wide (50.8 mm) coating of thermosetting adhesive. The outer polar cap, constructed from gore material and thus having the same optical properties as the rest of the inflatable sphere, was 40 inches (1.016 m) in diameter. This cap was centered over the inner cap and was bonded to the gores by a 3-inch-wide (76.2 mm) coating of adhesive. The outer polar cap was vented by 10 reinforced



1/16-inch-diameter (1.59 mm) vent holes (fig. 9) to preclude entrapment of air between the two polar caps.

In order to insure direct-current continuity between the aluminum coating of each gore and between the gores and the outer polar caps, two continuity rings were applied to the polar cap area of the inflatable sphere. The inner continuity ring, centered on the edge of the outer polar cap, was designed to insure electrical contact between the outer polar cap and each gore.

It consisted of a silver paint preparation covered with 1-inch-wide (25.4 mm), 0.5-mil-thick ( $1.27 \times 10^{-2}$  mm) PET tape. The outer continuity ring, designed to insure electrical contact between gores, was centered at a radial distance of 22.5 inches (0.572 m) from the center of the outer polar cap. It consisted of the silver-paint preparation covered by two-layer laminate. The first layer of the laminate was 1/4-inch-wide (6.38 mm), 0.2-mil-thick ( $5.08 \times 10^{-3}$  mm) strip of aluminum foil. The second layer, 1-inch-wide, 0.5-mil-thick aluminized PET, was bonded to the inner layer by the thermosetting, heat-sealable adhesive used in fabricating seams of the inflatable sphere.

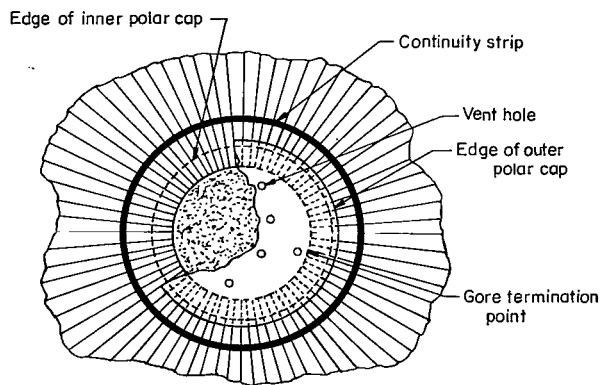


Figure 10.- PAGEOS dual polar cap configuration.

#### Folding, Inflation System Installation, and Packaging

During fabrication of the inflatable sphere, the material was pleat folded in the manner depicted in figure 11. Pleat folds were made every 9 inches (0.229 m) so that there would be five folds per gore. During pleat folding, and prior to the fabrication of the final seal, the inflation system consisting of  $10.0^{+0.2}_{-0.0}$  pounds mass ( $4.54^{+0.09}_{-0.00}$  kg) of benzoic acid and  $20.0^{+0.4}_{-0.0}$  pounds mass ( $9.08^{+1.8}_{-0.0}$  kg) of anthraquinone was dusted into the folds. The 10 pounds mass of benzoic acid and 5 pounds mass (2.27 kg) of anthraquinone were mixed and distributed uniformly over the interior surface of the

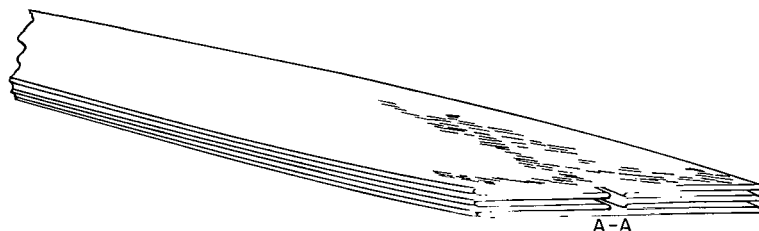


Figure 11.- PAGEOS pleat fold pattern.

sphere, within 26.2 feet (7.99 m) of the equator (equivalent to one-half of the surface area). The last 15 pounds mass (6.81 kg) of anthraquinone was distributed uniformly throughout the remainder of the sphere. After inflation system installation and completion of the final seal, the pleat-folded assembly was enclosed in a long plastic sleeve and evacuated to a design pressure of 250 torr (33.3 kN/m<sup>2</sup>) or less (approximately 50 torr (6.67 kN/m<sup>2</sup>) in actual practice) for 24 hours in order to compress the inflatable sphere prior to packaging. Next, each half of the pleat-folded material, beginning with the poles, was folded into one of the 26.5-inch-internal-diameter (0.673 m) canister halves in a rotated accordion pattern of varying fold lengths as shown in table II. (Fig. 12 is a top view looking down onto one-half of the folded and packaged satellite.) Completion of this operation within 1 hour after removal from the sleeve was required to maintain compression. Previously installed in each canister half was an octopus-shaped cotton fabric air wick designed to provide channels for the passage of air during evacuation from points within the canister and the sphere which were remote from the vacuum pumping system.

TABLE II.- ACCORDION-FOLD PATTERN

| Fold             | Accordion-fold length |            |       |       | Rotation,<br>deg | Fold                            | Accordion-fold length |            |       |       | Rotation,<br>deg |
|------------------|-----------------------|------------|-------|-------|------------------|---------------------------------|-----------------------|------------|-------|-------|------------------|
|                  | Individual            |            | Total |       |                  |                                 | Individual            |            | Total |       |                  |
|                  | inch                  | millimeter | inch  | meter |                  |                                 | inch                  | millimeter | inch  | meter |                  |
| a,b <sub>1</sub> | 24.0                  | 610        | 24.0  | 0.610 | 0 to 180         | 23                              | 25.0                  | 635        | 539.5 | 13.70 | 340 to 150       |
| 2                | 21.5                  | 546        | 45.5  | 1.16  | 180 to 10        | 24                              | 24.5                  | 622        | 564.0 | 14.33 | 150 to 320       |
| 3                | 19.0                  | 483        | 64.5  | 1.64  | 10 to 200        | 25                              | 24.0                  | 610        | 588.0 | 14.94 | 320 to 130       |
| 4                | 19.5                  | 495        | 84.0  | 2.13  | 200 to 30        | 26                              | 23.5                  | 597        | 611.5 | 15.53 | 130 to 300       |
| 5                | 20.0                  | 508        | 104.0 | 2.641 | 30 to 220        | 27                              | 23.0                  | 584        | 634.5 | 16.12 | 300 to 110       |
| 6                | 20.5                  | 521        | 124.5 | 3.162 | 220 to 50        | 28                              | 22.5                  | 572        | 657.0 | 16.69 | 110 to 280       |
| 7                | 21.0                  | 533        | 145.5 | 3.696 | 50 to 240        | 29                              | 22.0                  | 559        | 679.0 | 17.25 | 280 to 90        |
| 8                | 21.5                  | 546        | 167.0 | 4.241 | 240 to 70        | a <sub>30</sub>                 | 21.5                  | 546        | 700.5 | 17.79 | 90 to 270        |
| 9                | 22.0                  | 559        | 189.0 | 4.801 | 70 to 260        | 31                              | 21.0                  | 533        | 721.5 | 18.33 | 270 to 100       |
| 10               | 22.5                  | 572        | 211.5 | 5.372 | 260 to 90        | 32                              | 20.5                  | 521        | 742.0 | 18.85 | 100 to 290       |
| a <sub>11</sub>  | 23.0                  | 584        | 234.5 | 5.956 | 90 to 270        | 33                              | 20.0                  | 508        | 762.0 | 19.35 | 290 to 120       |
| 12               | 23.5                  | 597        | 258.0 | 6.553 | 270 to 80        | 34                              | 19.5                  | 495        | 781.5 | 19.85 | 120 to 310       |
| 13               | 24.0                  | 610        | 282.0 | 7.163 | 80 to 250        | 35                              | 19.0                  | 483        | 800.5 | 20.33 | 310 to 140       |
| 14               | 24.5                  | 622        | 306.5 | 7.785 | 250 to 60        | 36                              | 18.5                  | 470        | 819.0 | 20.80 | 140 to 330       |
| 15               | 25.0                  | 635        | 331.5 | 8.420 | 60 to 230        | 37                              | 18.0                  | 457        | 837.0 | 21.26 | 330 to 160       |
| 16               | 25.5                  | 648        | 357.0 | 9.068 | 230 to 40        | 38                              | 18.0                  | 457        | 855.0 | 21.72 | 160 to 350       |
| 17               | 26.0                  | 660        | 383.0 | 9.728 | 40 to 210        | 39                              | 18.0                  | 457        | 873.0 | 22.17 | 350 to 180       |
| 18               | 26.5                  | 673        | 409.5 | 10.40 | 210 to 20        | a <sub>40</sub>                 | 18.0                  | 457        | 891.0 | 22.63 | 180 to 0         |
| 19               | 27.0                  | 686        | 436.5 | 11.09 | 20 to 190        | a <sub>41</sub>                 | 18.0                  | 457        | 909.0 | 23.08 | 0 to 180         |
| 20               | 26.5                  | 673        | 463.0 | 11.76 | 190 to 0         | a <sub>42</sub>                 | 18.0                  | 457        | 927.0 | 23.55 | 180 to 0         |
| 21               | 26.0                  | 660        | 489.0 | 12.42 | 0 to 170         | a,c <sub>42</sub> $\frac{1}{2}$ | 9.0                   | 229        | 936.0 | 23.77 | 0 to 180         |
| 22               | 25.5                  | 648        | 514.5 | 13.07 | 170 to 340       |                                 |                       |            |       |       |                  |

aFold occurs at center line of fold pattern.

bNorth or South Pole of balloon.

cEquatorial fold.

After the completion of the accordion folding procedure, one of the canister halves was inverted. At this point, four overlapping smoke shields made of 3-mil-thick ( $7.62 \times 10^{-2}$  mm) laminated PET were placed along the periphery of the canister at the equatorial plane. The purpose of the smoke shields was to prevent grease from the canister O-ring seals and blowby resulting from the flexible linear shaped charge from striking the sphere during canister opening and balloon inflation. (Air wicks were dyed black and smoke shields were painted black so that they would not be seen in space.) After installation of the smoke shields, the canister halves were brought together until there was a uniform gap between them of  $0.2 \pm 0.05$  inch ( $5.08 \pm 1.27$  mm).

The spacecraft (canister plus sphere) was then placed in a vacuum chamber and was evacuated, at a rate not to exceed 4.0 torr per minute ( $533 \text{ N/m}^2$ ), to 0.08 to 0.10 torr ( $10.6$  to  $13.3 \text{ N/m}^2$ ). When outgassing from the inflatable sphere ceased to exceed 0.001 torr ( $0.133 \text{ N/m}^2$ ) per hour, the canister was remotely closed and an internal pressure not to exceed 0.9 torr ( $120.0 \text{ N/m}^2$ ) was maintained until deployment. The weight of the inflatable sphere and its inflation compounds was determined by weighing the canister and its accessories before and after balloon installation.

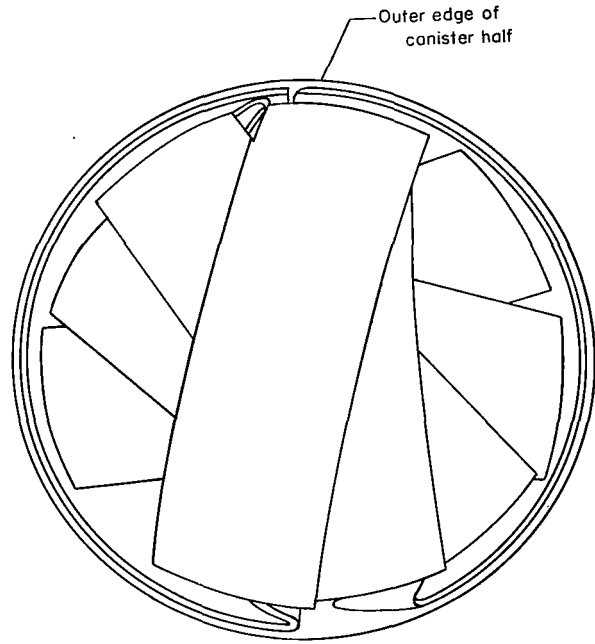


Figure 12.- Rotated, accordion-folded PAGEOS inflatable sphere installed in one-half of the canister.

#### Inflation System Distribution

The inflation system served a dual purpose. Its primary purpose was to inflate the balloon to full size in conjunction with the residual air remaining inside the folded sphere after canister evacuation. Also, it acted to prevent adhesion between PET surfaces of the folded sphere which could cause tearing during the inflation process. Of the two powders, benzoic acid is considered the primary inflatant because of its higher vapor pressure. Anthraquinone plays no significant role in the initial inflation process but, because of its low vapor pressure, remains in solid-vapor equilibrium for a relatively long time and acts as a sustainer to the inflated sphere. Since the folded balloon inflates to a cylindrical shape before becoming a sphere (because the accordion folds must be unfolded before the pleats can unfold), the pole tips are subjected to greater loading than the equatorial section. The inflation powders were therefore distributed within the inflatable sphere in the manner previously described, in order to produce a more uniform

skin stress over the entire balloon and to employ the antiadhesion properties of the inflatants to the fullest extent possible.

### PRODUCTION QUALIFICATION TESTS

Because the state of the art of inflatable sphere technology was not well defined prior to the start of the PAGEOS Project, a rigorous set of production and qualification tests was instituted to permit good quality control in the fabrication of PAGEOS I balloons. It is expected that the following description and presentation of the results of the various gore, tape, and seam tests will permit a reduction in the number of these tests necessary in future PAGEOS-type flight projects.

#### Gore Testing

Gore testing for PAGEOS inflatable sphere assemblies consisted of a sampling procedure involving seven distinct types of tests. Samples for testing of basic material properties were taken from a test area adjacent to the ends of each gore blank. When the rolled PAGEOS I material passed visual inspection in sufficient lengths to form two or more continuous gore blank lengths, the samples in each test area were permitted to represent the gores to either side, as shown in figure 13. Where visual inspection produced only one gore length, samples were taken from each end of the gore blank. Because of the nonuniform orientation of PET, mechanical properties tests were conducted on samples taken from both longitudinal (machine) and transverse roll directions (M.D. and T.D.). Samples were also taken from the center and edges of each gore blank.

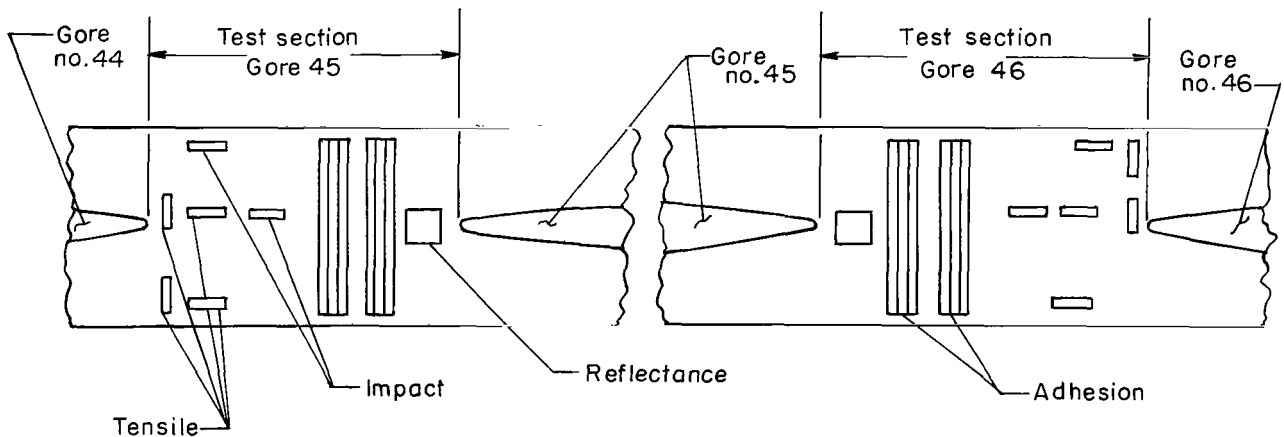


Figure 13.- Schematic layout for material testing of PAGEOS aluminized PET.

Eight samples representative of each gore were tested for ultimate tensile strength by use of a constant crosshead-rate tension testing machine with a load cell of 50 pounds force (222 N) maximum capacity. The samples, whose test sections were 5 inches (127.0 mm) by 1 inch (25.4 mm), were pulled at a crosshead speed of 2 inches per minute (0.85 mm/sec). To be acceptable for use in a PAGEOS I inflatable sphere, all specimens representative of a gore were required to have an ultimate tensile strength in excess of 18 000 pounds per square inch ( $1.24 \times 10^8$  N/m<sup>2</sup>).

By using a specimen-in-head impact tester, the tensile impact strength of four samples representative of each gore was determined. The samples were cut to a size 3 inches (76.2 mm) in length and 1 inch (25.4 mm) in width and then folded in half along the 3-inch axis. The minimum acceptable value necessary for inclusion into a sphere was 2480 inch-pounds per cubic inch ( $1.7 \times 10^7$  N/m<sup>2</sup>).

Two samples representative of each gore were tested for total integrated solar reflectance of the aluminum surface between 3600 and 7000 angstroms. A double-beam recording spectrophotometer with an integrating sphere was used which employed a highly specular silvered mirror as a reference standard. Samples were required to have a weighted solar reflectance between 83 and 90 percent to be acceptable. The same samples were also tested indirectly for specularly on the same instrument by measurement of the diffuse component of the total reflectance. A specular component in excess of 93 percent was required.

The resistivity of the aluminized surface of the PAGEOS I material was routinely measured in order to determine whether the coating was sufficiently thick to protect the PET substrate from ultraviolet degradation. One sample per test section was placed in a testing jig and the electrical resistance of an area 6 inches long (152.4 mm) and 1 inch wide (25.4 mm) was measured. A resistivity of 1 ohm or less per square inch was required for acceptance. (1 ohm per square inch is approximately equal to 2000 angstroms.)

Because of a problem encountered during the fabrication of the static inflation test prototype (discussed in greater detail in a following section), two tests were instituted, beginning with the fabrication of the deployment test sphere, which were designed to measure the adhesion properties of the plastic surface of the PAGEOS material. In the first test, designated canister-simulation adhesion testing, six samples representative of each gore were subjected to an environment designed to oversimulate the environment of the packaged sphere. Samples 50 inches long (1.27 m) and 2 inches wide (50.8 mm) were accordion folded into a 2-inch by 2-inch configuration and placed in a platen press for 3 hours at a temperature of 150° F (65.6° C) and a static loading of 20 pounds per square inch ( $1.38 \times 10^5$  N/m<sup>2</sup>). After being subjected to this environment, the samples were placed in a constant crosshead-rate tension testing machine with a load cell of 2000 grams

force (19.6 N) maximum capacity and the accordion folds were peeled apart at a cross-head speed of 50 inches per minute (1.27 m/min). Acceptance required that the peel force necessary to separate any of the 25 folds of any of the representative samples not exceed 40 grams per inch of width (1.51 g/mm) and, additionally, that the sample should not tear during the entire peeling process. In the second test, designated sealing-wheel adhesion testing, six samples representative of each gore were subjected to an environment designed to simulate the gore-sealing operation. Two strips of fabrication material, each 50 inches long and 2 inches wide, were pressed together, plastic side to plastic side, and placed under a 1-inch-wide (25.4 mm) sealing wheel at 340° F (171° C), a pressure of 160 pounds per square inch ( $1.10 \times 10^6$  N/m<sup>2</sup>) and a sealing speed of 6 feet per minute ( $3.048 \times 10^{-2}$  m/sec). These samples were then peeled apart in a manner similar to that described above for canister-simulation adhesion. Acceptance criteria were the absence of tearing and a peel force not to exceed 15 grams per inch of width (0.59 g/mm).

In all, 881 gores were cut for the fabrication of PAGEOS I and its prototypes, backups, and spares. In order to evaluate the properties of the basic fabrication material in a reasonable amount of time, the results of testing on every tenth gore were used for this report. These results are shown in table III in the form of mean value and standard deviation. The validity of choosing a 10-percent sample lies in the large number of tests conducted in each test category, as revealed by the fact that the maximum difference between sample and total population means, for a 95-percent confidence factor, are all relatively small. Also shown in table III are the mean-value and standard-deviation results for the flight sphere. Comparison of the two sets of data indicates that the material used in the flight sphere was, with the exception of surface adhesion properties, typical of all material used in the testing and fabrication of all the inflatable spheres. The lower standard deviations of the flight sphere adhesion test data are a reflection of positive action to exclude from it material with high-peel-force values. Not reflected in table III is the nonuniformity of tensile-strength test values for center and edge samples which varied from roll to roll. This phenomenon did not occur in impact testing and is not presently understood.

The maximum and minimum values of all mechanical, optical, and surface properties test data for PAGEOS I are plotted in figures 14 and 15 on a gore-by-gore basis as an indication of the tolerances which can be readily held on a flight-configuration inflatable sphere.

In addition to the test described, two other qualification tests were performed on each potential gore. The first of these was a measurement of material thickness by use of a motorized micrometer which exerted a near-constant pressure on the sample of  $25 \pm 2$  pounds per square inch ( $1.75 \pm 0.14 \times 10^5$  N/m<sup>2</sup>). The criterion for acceptability was a thickness of  $0.50 \pm 0.05$  mil ( $1.27 \pm 0.13 \times 10^{-2}$  mm). All material purchased for

TABLE III.- MATERIAL TEST RESULTS

[M.D. denotes machine direction; T.D. denotes transverse roll direction]

| Materials test  | Sampling of tests performed on all gores |   |                               | Flight sphere gores                                   |
|---|--|---|-------------------------------|---|
|   | Number of samples                        | Mean value $\pm$ one standard deviation               | $ x - \mu $<br>P = 0.95*      | Mean value $\pm$ one standard deviation               |
| Ultimate tensile strength, M.D., lb/in <sup>2</sup> (N/m <sup>2</sup> )   | 329                                      | 24 900 $\pm$ 3000<br>(17.2 $\pm$ 2.1 $\times 10^7$ )  | 300<br>(2.1 $\times 10^6$ )   | 24 600 $\pm$ 3400<br>(17.0 $\pm$ 2.3 $\times 10^7$ )  |
| Ultimate tensile strength, T.D., lb/in <sup>2</sup> (N/m <sup>2</sup> )   | 328                                      | 28 600 $\pm$ 3800<br>(19.7 $\pm$ 2.6 $\times 10^7$ )  | 400<br>(2.8 $\times 10^6$ )   | 28 100 $\pm$ 3700<br>(19.4 $\pm$ 2.6 $\times 10^7$ )  |
| Tensile impact strength, M.D., in-lb/in <sup>3</sup> (N/m <sup>2</sup> )  | 160                                      | 6160 $\pm$ 1700<br>(4.25 $\pm$ 1.2 $\times 10^7$ )    | 300<br>(2.1 $\times 10^6$ )   | 6080 $\pm$ 1400<br>(4.19 $\pm$ 0.97 $\times 10^7$ )   |
| Tensile impact strength, T. D., in-lb/in <sup>3</sup> (N/m <sup>2</sup> ) | 160                                      | 4800 $\pm$ 1200<br>(3.31 $\pm$ 0.83 $\times 10^7$ )   | 200<br>(1.4 $\times 10^6$ )   | 4800 $\pm$ 960<br>(3.31 $\pm$ 0.66 $\times 10^7$ )    |
| Canister-simulation adhesion, grams/inch of width (g/mm)                  | 374**                                    | 3.9 $\pm$ 6.8<br>(0.15 $\pm$ 0.27)                    | 0.7<br>(0.3)                  | 6.6 $\pm$ 3.5<br>(0.26 $\pm$ 0.14)                    |
| Sealing-wheel adhesion, grams/inch of width (g/mm)                        | 390***                                   | 2.1 $\pm$ 1.6<br>(0.082 $\pm$ 0.063)                  | 0.2<br>(0.08)                 | 2.3 $\pm$ 1.3<br>(0.091 $\pm$ 0.051)                  |
| Resistivity of aluminum, ohms/in <sup>2</sup> (ohms/mm <sup>2</sup> )     | 164                                      | 0.70 $\pm$ 0.15<br>(1.1 $\pm$ 0.23 $\times 10^{-3}$ ) | 0.02<br>(3 $\times 10^{-5}$ ) | 0.77 $\pm$ 0.09<br>(1.2 $\pm$ 0.14 $\times 10^{-3}$ ) |
| Total reflectance of aluminum, percent                                    | 159                                      | 89.15 $\pm$ 0.43                                      | 0.07                          | 89.32 $\pm$ 0.39                                      |
| Specular component of aluminum reflectance, percent                       | 159                                      | 96.59 $\pm$ 0.84                                      | 0.13                          | 96.98 $\pm$ 0.78                                      |

\*95-percent confidence that the absolute value of the difference between sample and total population means does not exceed the value given.

\*\* Original analysis of the data yielded a result of 4.3  $\pm$  25.4 grams per inch (0.17  $\pm$  1.00 g/mm) of width. One sample whose test value (300 g/in. (11.8 g/mm) width) exceeded the mean value by more than 3 $\sigma$  was then excluded from consideration. Recomputation gave the results shown.

\*\*\* Original analysis of the data for this test yielded a result of 3.2  $\pm$  6.3 grams per inch (0.13  $\pm$  0.25 g/mm) of width. Twelve samples whose test values exceeded the mean value by more than 3 $\sigma$  were then excluded from consideration. Recomputation gave the results shown.

the fabrication of the inflatable spheres met this qualification. A second test was a qualitative check on the adhesion of the aluminum coating to the PET substrate. In this test, a piece of adhesive cellophane tape was placed on a roller and the roller was rubbed a number of times across the surface of the test area. If any of the aluminum was separated from its substrate by the cellophane tape, the gore was rejected. Future users of aluminized PET should give consideration to seeking a more quantitative measurement of aluminum adhesion to its substrate.

### Tape Testing

Each roll of tape intended for use as a seal on a PAGEOS I inflatable sphere was tested for thickness, tensile-impact strength, and peel strength in a manner similar to those used in the testing on the basic material or seams. The qualification requirements were also the same. Tapes were stored at 0<sup>o</sup> C prior to use and once permitted to attain

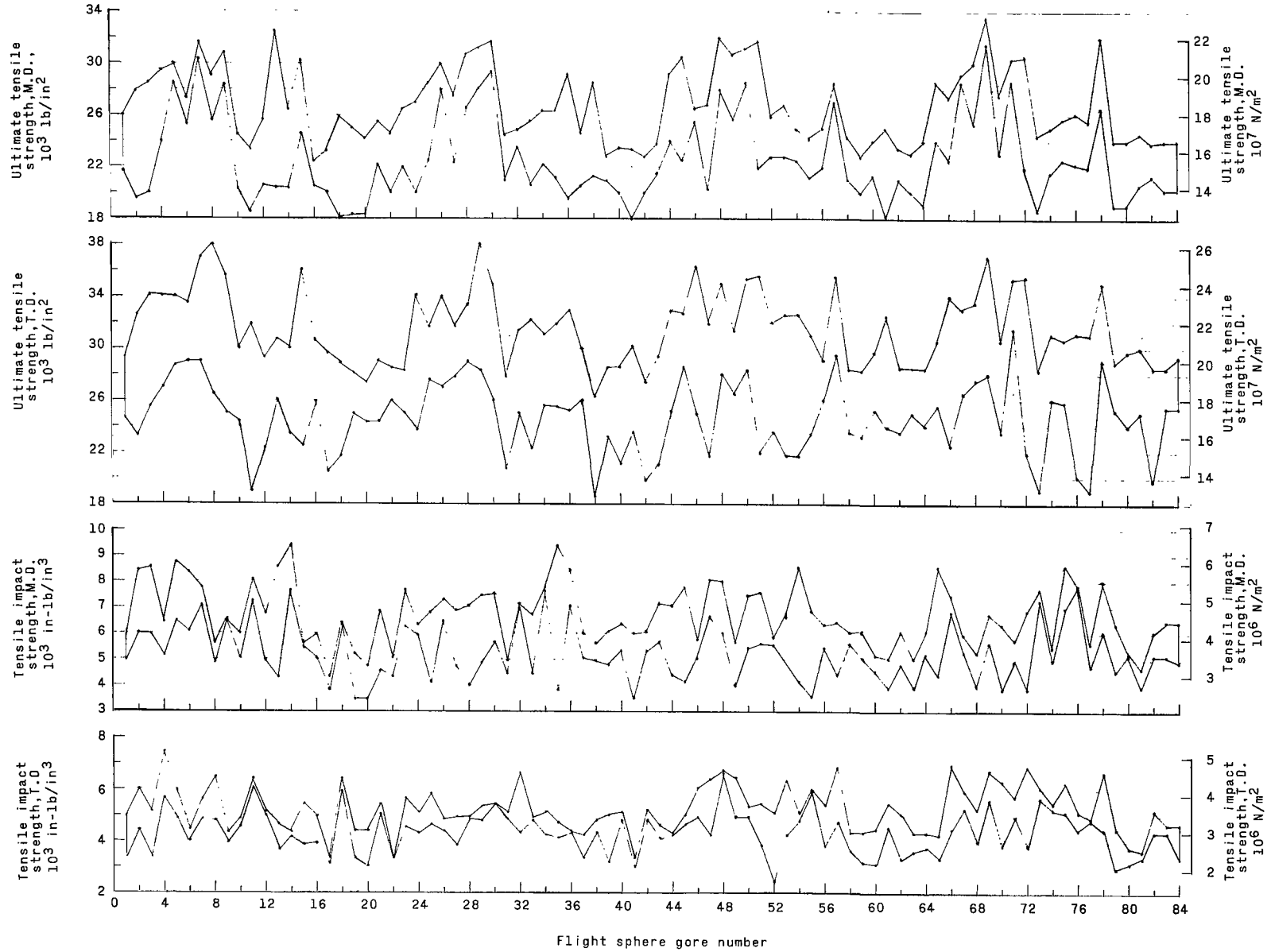


Figure 14.- Maximum and minimum values of mechanical properties test data for each gore of the PAGEOS flight sphere. (M.D. denotes machine direction and T.D. denotes transverse roll direction.)



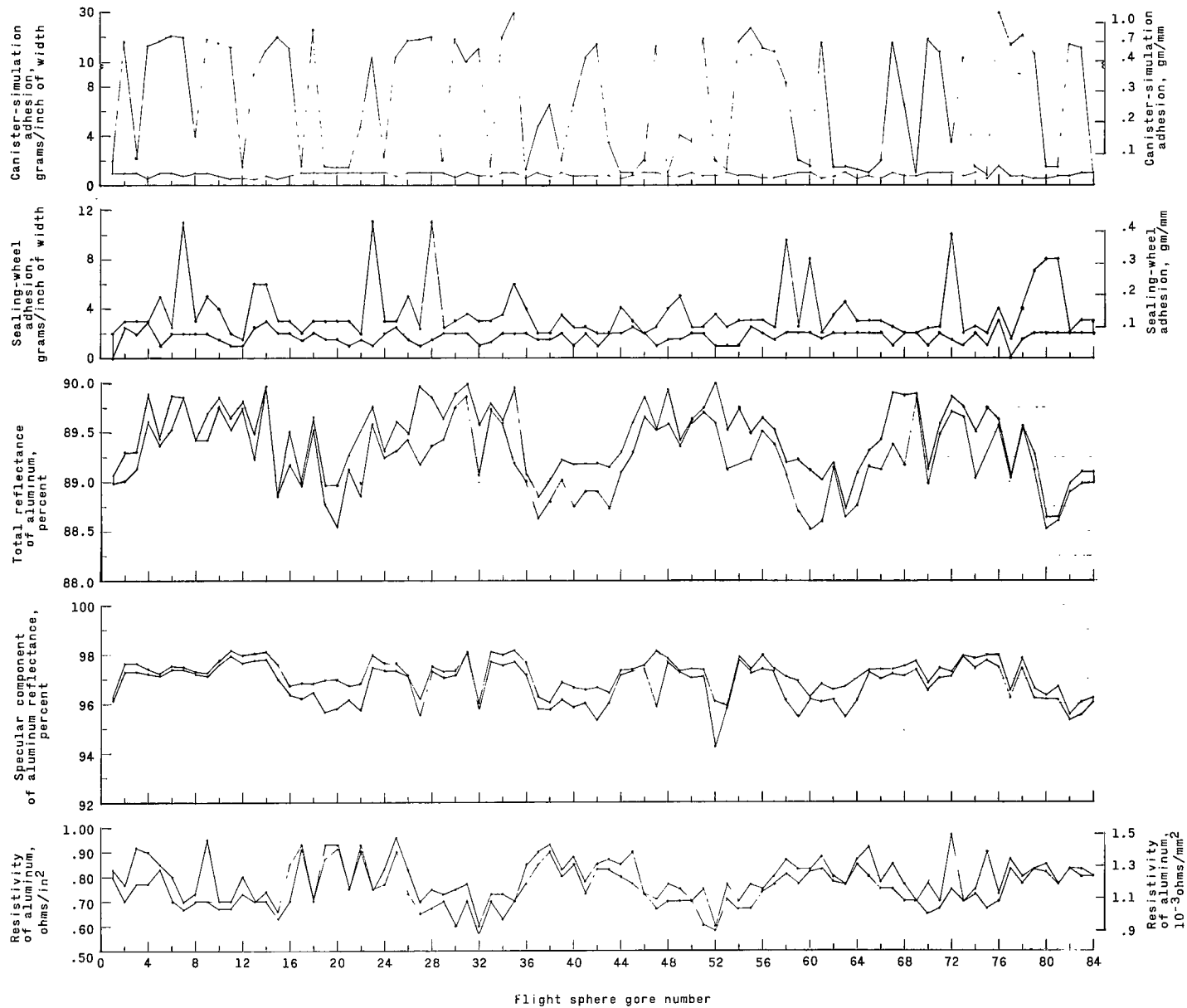


Figure 15.- Maximum and minimum values of optical and surface properties test data for each gore of the PAGEOS flight sphere.

room temperature were not refrigerated again. If not used within 24 hours after removal from the refrigerator, the tapes were discarded. In addition, no tapes to which the adhesive had been applied more than 30 days prior to intended use were permitted to be used in the inflatable sphere fabrication.

### Seal Testing

If a gore blank satisfactorily passed all its basic material tests, it was then cut to shape and sealed into a balloon. A section of the gore blank was kept with the gores. This section plus an extension of the sealing tapes were used in the formation of samples for seal testing (fig. 16). Four different tests were used to evaluate seal strength. All seal samples were permitted to cure for at least 24 hours before testing.

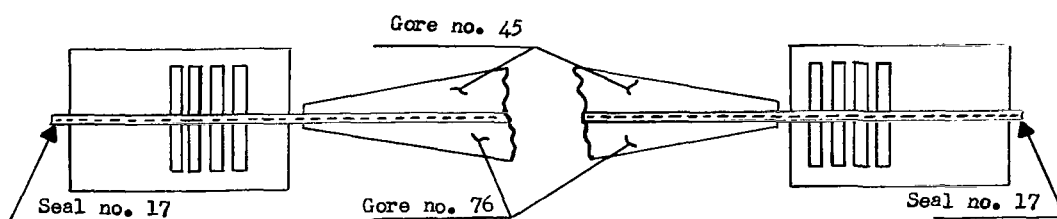


Figure 16.- Layout for seal testing of PAGEOS aluminized PET.

Two 1-inch-wide (25.4 mm) samples from each gore seam were subjected to flexure testing by wrapping them 180° around a 1/4-inch-diameter (6.35 mm) dowel 10 times in liquid nitrogen and then 10 times in room temperature air. The sequence was repeated five times. The sample was then tested for ultimate tensile strength, the minimum requirement for acceptance being 18 000 pounds per square inch (124 MN/m<sup>2</sup>).

Two 1-inch-wide (25.4 mm) samples from each gore seam were subjected to thermal shock by being alternately dipped for 3 seconds into 100° C air and liquid nitrogen. The sequence was repeated 50 times. The sample was then tested for ultimate tensile strength, the minimum requirement for acceptance being 18 000 pounds per square inch (124 MN/m<sup>2</sup>).

Seam creep was determined by the application of a static load of 2000 pounds per square inch (138 MN/m<sup>2</sup>) to two 1-inch-wide (25.4 mm) samples from each gore seam for a minimum of 12 hours at a temperature of 150° C. Seam creep in excess of 0.020 inch (0.508 mm) constituted a failure.

Tests were also conducted to determine the ability of the seams to withstand a peel force. Longitudinally cut samples were mounted in the jaws of the tension-testing machine so that a 180° peel took place when the crossheads moved apart. The seals were required to withstand a peel force of 1.3 pounds per inch (0.228 N/mm) of seal width.

Any seal which failed to pass all the tests listed was bitaped and the tests were conducted again on the bitaped specimens. Failure of the bitaped specimens to pass the qualification tests necessitated removal and replacement of the gore and tape. Gore removal proved to be unnecessary in the flight sphere. The following limitations were placed on seal repairs:

(a) The maximum continuous repair length per seal was not permitted to exceed 8 feet (2.44 m).

(b) The maximum total repair length per seal (excluding gore replacement) was not permitted to exceed 15 feet (4.57 m).

(c) Cuts for dimensional repairs were made 30 percent longer than the defect length on either end.

(d) Splice plate repair tapes were extended a minimum of 2.0 inches (50.8 mm) beyond the cut length on either end of the out-of-tolerance length.

For the seal tests, the data for every seventh seal were evaluated for this report. The mean value and standard deviation of these sample groups are shown in table IV. Also shown is the maximum difference between sample and total population means for 95-percent confidence factor, and the results of seal testing for the flight sphere. As in the material test results (see table II), both the sample data and the flight sphere data have a high probability of being representative of all seals formed of the same materials.

The maximum and minimum values of all seam properties test data for the PAGEOS I flight sphere are plotted in figure 17.

TABLE IV.- SEAL TEST RESULTS

| Seam tests  | Sampling of tests performed on all seams |  |                             | Flight sphere seams                                  |
|---|--|--|-----------------------------|--|
|   | Number of samples                        | Mean value $\pm$ one standard deviation              | $ x - \mu $<br>P = 0.95*    | Mean value $\pm$ one standard deviation              |
| Ultimate tensile strength after flexure, lb/in <sup>2</sup> (N/m <sup>2</sup> )       | 144                                      | 26 800 $\pm$ 3300<br>(18.5 $\pm$ 2.3 $\times 10^7$ ) | 500<br>(3.4 $\times 10^6$ ) | 26 300 $\pm$ 3000<br>(18.1 $\pm$ 2.1 $\times 10^7$ ) |
| Ultimate tensile strength after thermal shock, lb/in <sup>2</sup> (N/m <sup>2</sup> ) | 144                                      | 26 700 $\pm$ 3300<br>(18.4 $\pm$ 2.3 $\times 10^7$ ) | 500<br>(3.4 $\times 10^6$ ) | 26 000 $\pm$ 2700<br>(17.9 $\pm$ 1.9 $\times 10^7$ ) |
| Seam creep, inch (mm)   | 144                                      | 0.007 $\pm$ 0.005<br>(0.2 $\pm$ 0.1)                 | 0.001<br>(0.03)             | 0.009 $\pm$ 0.005<br>(0.2 $\pm$ 0.1)                 |
| Seam peel, lb/inch (N/mm) of width  | 144                                      | 2.6 $\pm$ 1.3<br>(0.45 $\pm$ 0.23)                   | -----                       | 3.1 $\pm$ 0.9<br>(0.54 $\pm$ 0.16)                   |

\*95-percent confidence that the absolute value of the difference between sample and total population means  $|x - \mu|$  does not exceed the value given.

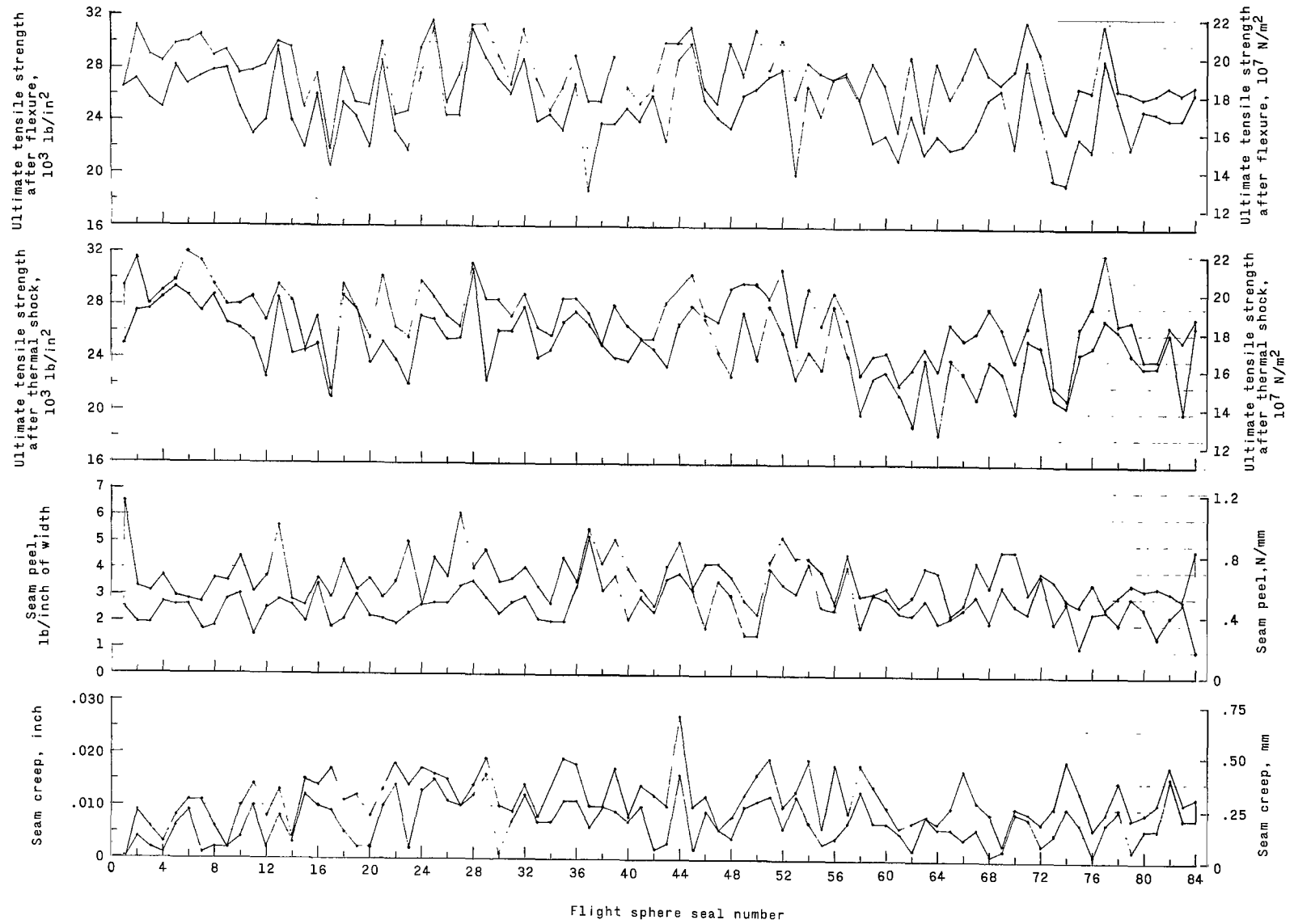


Figure 17.- Maximum and minimum values of mechanical properties test data for each seal of the PAGEOS flight sphere.

## SPECIAL TESTS

### Static Inflation Test

A static inflation test was conducted on a PAGEOS I prototype sphere in August 1965. This sphere was modified in advance of the test by the addition of ducts at each pole which permitted intake and exit of gases for inflation and lift. The prototype also differed from the other spheres in the lack of inflation powders and vent holes. A view of the fully inflated static inflation test sphere is shown in figure 1.

The objectives of the static inflation test were threefold:

- (1) To determine the ultimate strength of the sphere
- (2) To determine the amount of seam creep
- (3) To determine its sphericity from diameter measurements.

The static inflation test sphere was subjected to a series of gradual increases in skin stresses and long hold times at these stresses. For example, skin stresses of 700, 2000, 3000, and 4000 psi (4.83, 13.7, 20.7, and 27.6 MN/m<sup>2</sup>) were held for 5 hours each whereas stresses of 6000 psi (41.4 MN/m<sup>2</sup>) and 8000 psi (55.2 MN/m<sup>2</sup>) were held for 1 hour. The sphere ruptured after being at 10 000 psi (68.9 MN/m<sup>2</sup>) skin stress for 5 minutes. No creep was observed in the seam test areas during or after the test.

The polar diameter was measured at the various skin stress levels between 700 psi (48.3 MN/m<sup>2</sup>) and 8000 psi (55.2 MN/m<sup>2</sup>) by means of a 5-mil-thick (0.127 mm) graduated PET tape suspended inside the sphere. Equatorial diameter measurements were performed by use of eight theodolites stationed around the sphere, as shown in figure 18. The theodolites were simultaneously sighted on the center of bright orange spheres attached to cones which were, in turn, attached to the equator of the PAGEOS I prototype at eight evenly spaced points. Since the combined length of two of these attachments was approximately 2/3 foot (0.203 m), the theodolites were spaced 100.667 feet (30.6833 m) apart. Equatorial diameter measurements were made by having two theodolites simultaneously sight on one cone; thereby, for example, the coordinates of points C and G were determined. By use of an equation of the form

$$\sqrt{(x - x_G)^2 + (y - y_G)^2}$$

the length CG was determined. All other equatorial diameters were determined in a similar manner.

A plot of the average values of both polar and equatorial diameter measurements as a function of sphere skin stress is shown in figure 19. The flagged marks at each data point indicate the maximum and minimum readings recorded for that point.

Readings were taken at both the start and end of the 5-hour hold time at the 4000 psi (27.6 MN/m<sup>2</sup>) skin stress level. The marked difference in polar diameter measurements, and the smaller difference in equatorial diameter measurements, obtained at the start and end of this skin stress level are attributable to large differences in the total lift of the sphere at these times. As seen in figure 19, the polar and equatorial diameters increased gradually with sphere skin stress, although their absolute values were both lower than the theoretically predicted elongation of PET (shown as a dotted line). The theoretical prediction was based on a 100-foot-diameter (30.48 m) sphere under no-load conditions. Of significance is the fact that the empirical growth of the sphere can be related directly to its material properties, and thereby gives confidence in the measurements.

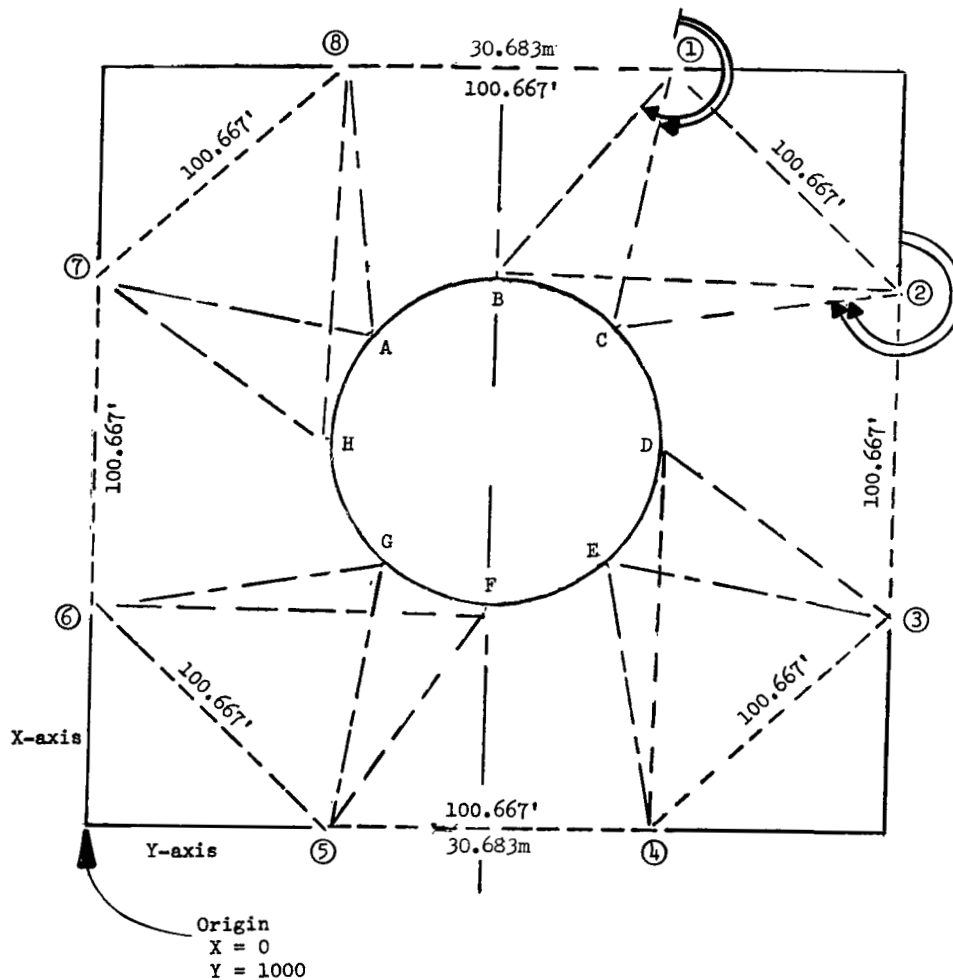


Figure 18.- Theodolite station layout for PAGEOS static inflation test equatorial diameter measurements.

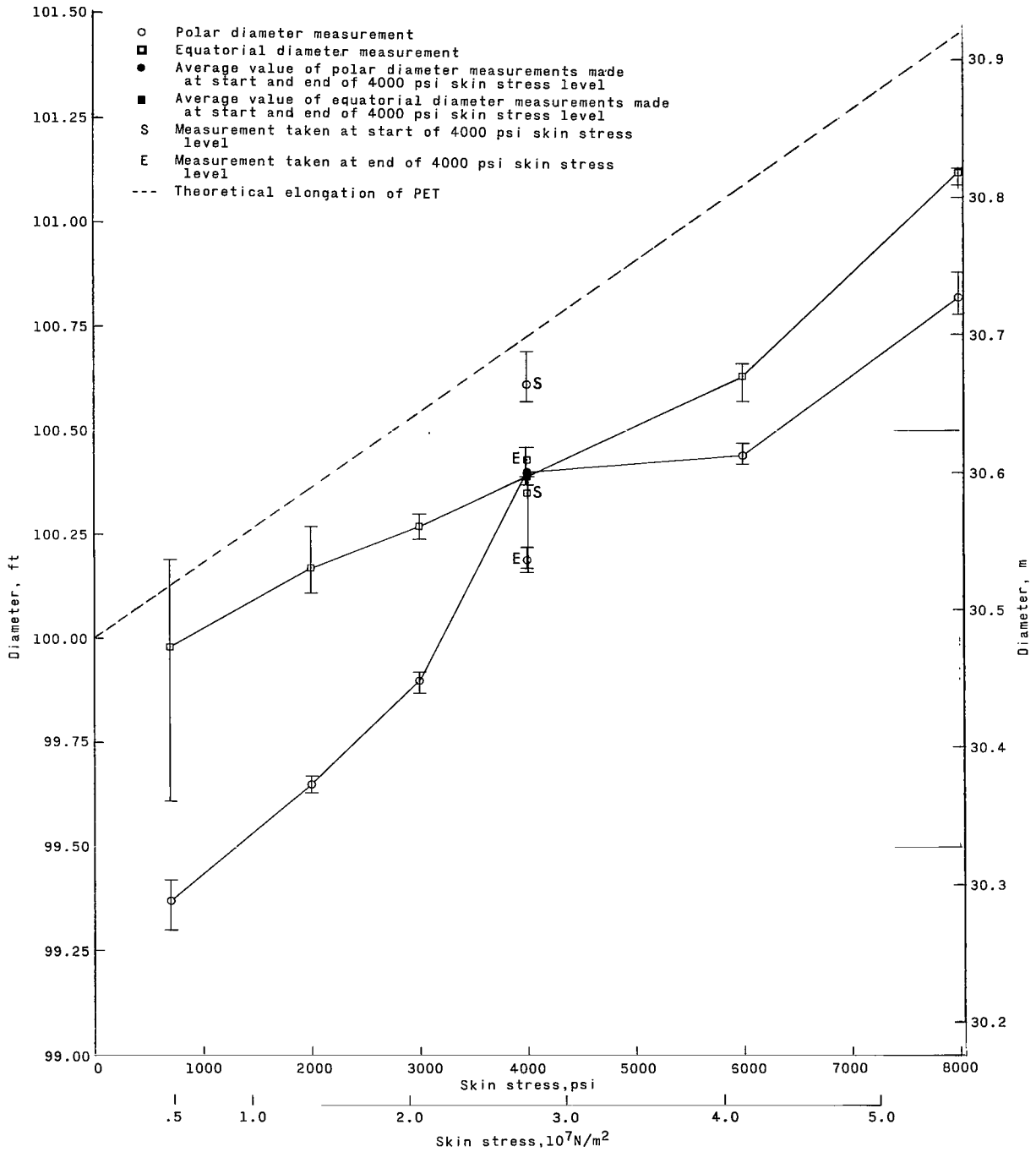


Figure 19.- Variation of polar and equatorial diameters of the PAGEOS static inflation test sphere as a function of skin stress.

The discovery of adhered areas during the fabrication and testing of the static inflation test prototype resulted in the use of chemical treatment on all later spheres. Additionally, observation and analysis of the initial point of rupture of the test sphere revealed a misalignment of the gore-cutting template, as a result of which, more frequent template tolerance checks were instituted.

### Deployment Test

A deployment test of a PAGEOS I prototype spacecraft (inflatable sphere plus canister) was conducted in March 1966 in the 60-foot vacuum sphere at the Langley Research Center. The purposes of this test, as they apply to the inflatable sphere, were to:

- (1) Verify that the canister halves were separated with a velocity sufficient to preclude collision with the inflatable sphere during deployment
- (2) Determine the deployment velocity of the sphere
- (3) Verify that the canister opening system did not damage the inflatable sphere
- (4) Assess qualitatively the techniques employed in sphere fabrication and packaging
- (5) Assess qualitatively the inflation process and thereby, the inflation system.

The spacecraft was hung from a beam in a manner which placed it at the center of the vacuum chamber. The chamber was evacuated to  $4 \times 10^{-4}$  torr ( $5.332 \times 10^{-2}$  N/m<sup>2</sup>) prior to the test.

A study of motion pictures taken during the test revealed that:

- (1) The velocity with which the inflatable sphere deployed was 18 feet per second (5.48 m/sec), equator to pole
- (2) The separation velocities of the canister halves were 28 feet per second (8.53 m/sec) (for 21.0 pounds mass (9.53 kg)) and 30 feet per second (9.14 m/sec) (for 18.3 pounds mass (8.31 kg))
- (3) At no time did the inflating sphere come in contact with either of the canister halves.

Some sequential views of the sphere during the test are shown in figure 20.

Inspection of the balloon after the test revealed the presence of vacuum grease, powder impingement, smoke stains, and canister thermal control tape on the balloon surface resulting from shaped charge detonation. Minor redesign of the protective smoke shield and application of the thermal control tape to the equatorial flange of the canister were made to preclude these occurrences during the actual deployment in space.



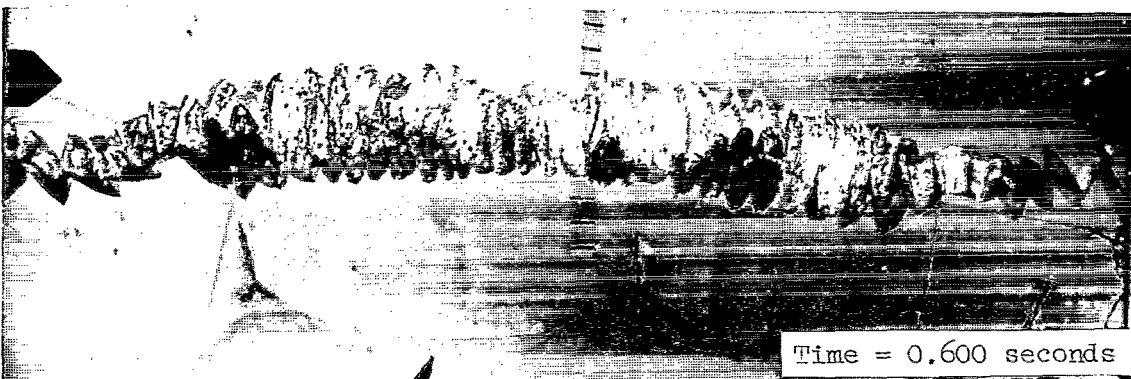
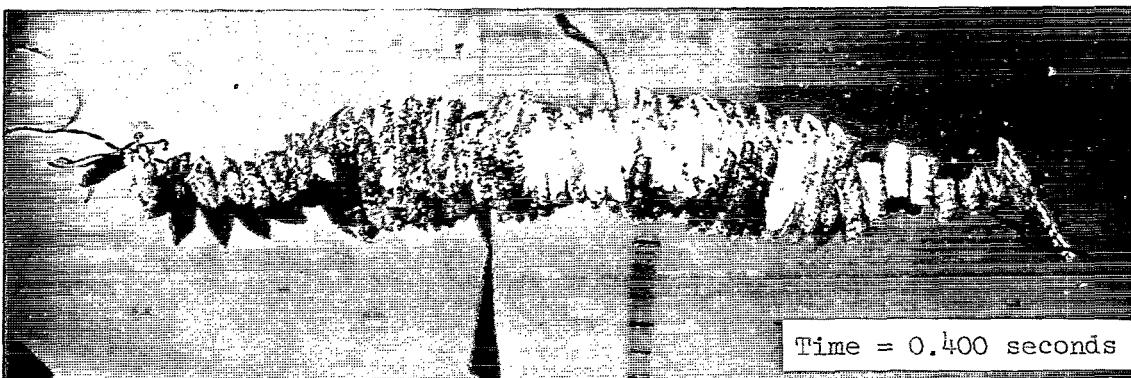
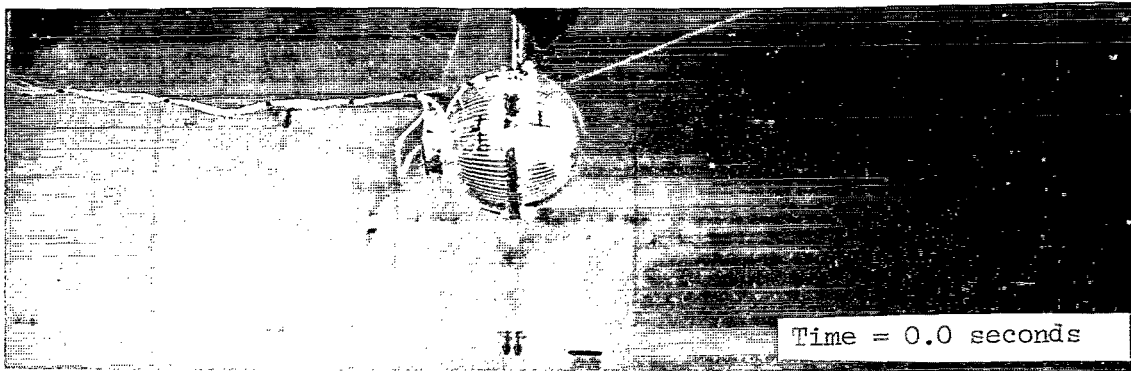


Figure 20.- Deployment of PAGEOS I prototype in the 60-foot vacuum sphere at the Langley Research Center.

Five burn holes found in the sphere were found to have been caused by contact with hot electrical elements from photographic lights broken by the impact of the canister's explosive opening system. In addition, a number of minor defects in sphere fabrication and packaging were found and stricter quality control measures and process changes were instituted to prevent their recurrence.

The inflatable sphere was deployed with the desired orientation and elongation rates. Only a small amount of pleat-fold inflation occurred during the balloon's fall from the vacuum chamber's center to restraining nets placed above the chamber's floor. (See fig. 20.) After the balloon reached the net, a moderate amount of pleat-fold inflation occurred, the maximum diameter of the largest bubble being approximately 5 feet (1.52 m). This production of bubbles was attributed to heating of the inflation powders by the photographic lights. The inflation process and the inflation system were therefore adjudged to be satisfactory for flight.

#### Silver Paint Study

A third test series was initiated to evaluate the capabilities of a commercial silver paint preparation as a dc continuity strip in the polar cap areas of the PAGEOS I inflatable sphere assemblies, and to study the possible deleterious effects of this preparation on the PAGEOS I fabrication material. The silver paint preparation consisted of a polyester vehicle, a solvent to dissolve the polyester, and a silver pigment. Curing of this preparation resulted in the evaporation of the solvent and left the polyester vehicle and the silver pigment. The PAGEOS I silver paint preparation was applied to various seamed samples and electrical resistance measurements were made across the sample joint before and after testing.

Silver paint strips were applied to a total of 34 seam samples which were subjected to flexure, thermal shock, and seam creep tests similar in all respects to those performed on samples taken from PAGEOS I inflatable sphere seams, except that seam creep tests were conducted at 3000 psi ( $20.7 \text{ MN/m}^2$ ) skin stress and  $240^\circ \text{ F}$  ( $115.6^\circ \text{ C}$ ) for at least 24 hours. The results of these tests showed that the PAGEOS I silver paint preparation withstood this rigorous testing with a maximum increase in resistance of approximately 10 percent.

Ten additional samples were subjected to a vacuum of  $3 \times 10^{-7}$  torr ( $4.0 \times 10^{-5} \text{ N/m}^2$ ) for 114 hours at room temperature. In all cases, the samples lost less than 1 percent of their original weight and increased in electrical resistance less than 3 percent.

In a further series of tests, samples were subjected for at least 24 hours to temperatures up to  $200^\circ \text{ C}$  (1) at atmospheric pressure, (2) in a vacuum of 15 to 50 microns ( $2.00$  to  $6.67 \text{ N/m}^2$ ), and (3) in an oxygen-enriched atmosphere with a pressure of

16.2 pounds per square inch ( $11.2 \text{ MN/m}^2$ ), with no detectable change in electrical resistance. Elevated temperatures did, however, produce discoloration of the paint from silver to beige, and above  $200^\circ \text{C}$ , caused severe embrittlement of the paint strip.

The last series of tests consisted of determining the tensile strength of painted samples, 12 of which were of the basic fabrication material and 8 of which were seamed. In all cases, the tensile strength of the painted samples exceeded that of the control samples.

In summary, the silver paint preparation maintained its low electrical resistance despite subjection to extremes of temperature, pressure, and mechanical loading, and appeared to have no degrading effect on the PAGEOS I material.

#### Transmission Characteristics

The manner in which the solar absorptance of PAGEOS I aluminized PET is calculated from reflectance data depends heavily on the validity of the assumption that the transmission of light through the material is zero. In order to verify this assumption, the percent transmission of five samples of PAGEOS I material was determined in the ultraviolet, visible, and infrared regions of the electromagnetic spectrum. A single-beam, hand-driven spectrophotometer was employed. The results indicated near-zero transmission between 2200 angstroms and 8000 angstroms and less than 1-percent transmission between 8500 angstroms and 10,000 angstroms.

#### Seam Creep Tests

During the course of the program, seam creep tests were conducted to study the effect of various combinations of static load, temperature, and time under load on PAGEOS I seals.

Samples were prepared by butting together two pieces of 4-inch-wide (101.6 mm) PAGEOS I material with a 1-inch-wide (25.4 mm) thermosetting adhesive tape. Tests were conducted in a vacuum oven at 10 to 50 micrometers ( $1.33$  to  $6.67 \text{ N/m}^2$ ) with the sample uniaxially loaded transverse to the seam direction. The maximum oven temperature was  $205^\circ \text{C}$ .

Results for tests of 23 to 30 hours duration are given in table V. The words "complete failure" indicate that tearing of the samples in the seam area produced separation of the two pieces of parent material.

As a check on the data obtained at a temperature of  $205^\circ \text{C}$  and a skin stress of 1000 pounds per square inch ( $6.89 \text{ MN/m}^2$ ), a further series of tests was conducted. Of the three samples tested, one failed completely in 24.5 hours whereas the other two failed completely in 42.3 and 45.2 hours. An additional sample was then tested at a

stress of 750 pounds per square inch (5.17 MN/m<sup>2</sup>) and a temperature of 196° C, the maximum stress and temperature to which the seams of the passive geodetic satellite are subjected after inflation. The test was terminated after 274 hours, the amount of creep varying from a minimum of 0.045 inch (1.14 mm) to a maximum of 0.104 inch (2.64 mm).

This latter set of tests emphasizes the fact that extreme care must be exercised in the selection of an inflation system for satellites of the PAGEOS type, since the margin between sufficient and excessive skin stress appears to be very small at equilibrium temperatures near 200° C.

TABLE V.- SHORT-TERM SEAM CREEP TESTS

| Skin stress        |                   | Temperature,<br>°C | Maximum creep                 |             |
|--------------------|-------------------|--------------------|-------------------------------|-------------|
| lb/in <sup>2</sup> | N/m <sup>2</sup>  |                    | thousandths<br>of an inch     | millimeters |
| 1000               | $6.9 \times 10^6$ | 205                | 0                             | 0           |
|                    |                   | 121                | 0                             | 0           |
|                    |                   | 144                | 0                             | 0           |
|                    |                   | 184                | 10                            | .25         |
|                    |                   | 205                | Complete failure in 5 hours   |             |
| 3000               | $2.1 \times 10^7$ | 121                | 0                             | 0           |
|                    |                   | 160                | 15                            | .38         |
|                    |                   | 174                | 18                            | .46         |
|                    |                   | 180                | 45                            | 1.1         |
|                    |                   | 189                | Complete failure in 13 hours  |             |
| 4000               | $2.8 \times 10^7$ | 121                | 0                             | 0           |
|                    |                   | 163                | 20                            | .51         |
|                    |                   | 176                | 25                            | .63         |
|                    |                   | 184                | Complete failure in 4 hours   |             |
| 4500               | $3.1 \times 10^7$ | 121                | 0                             | 0           |
| 4700               | $3.2 \times 10^7$ | 121                | 20                            | .51         |
| 5000               | $3.4 \times 10^7$ | 121                | 40                            | 1.0         |
| 6000               | $4.1 \times 10^7$ | 121                | Complete failure in 1.5 hours |             |

## PROBLEM AREAS AND SOLUTIONS

### Adhesion and Chemical Treatment

During the course of fabrication of the PAGEOS static inflation test sphere, it became apparent that under certain conditions of temperature and pressure, the PET used in inflatable sphere fabrication could adhere to itself with a force sufficient to cause tearing when attempts were made at separation by hand. Although no conclusive proof exists, it is believed that the adhesions were caused by the exudation of low molecular weight residues of the polymerization process to the surface of the film. It is further believed that this exudation occurred when the material was subjected to short-term, high-temperature, and vacuum conditions during the vapor deposition process. After an empirical evaluation of various cleaning fluids, a solution of a cationic detergent in freon was chosen with which to treat chemically the PAGEOS I material. The mechanism by which this solution prevented or reduced adhesion in PET is not presently understood. A laboratory-scale investigation of the effect of this chemical cleaning solution on the mechanical, optical, and surface properties of the PAGEOS I material was conducted concurrent with the building of a full-scale treating machine, and a study of the advisability of treating both sides of the material or the PET side only. The laboratory-scale investigation was conducted on 1-foot-wide (0.305 m) rolls of material with solution concentrations of 4.7, 7.8, and 9.4 parts per million (ppm) of the detergent in freon being used. The results of the laboratory-scale investigation showed that:

- (1) The PET side of the polymer film was the source of the undesirable adhesive
- (2) Chemical treatment with solution concentration of 4.7 ppm prevented adhesion from taking place
- (3) The optical, mechanical, and surface properties of the aluminized PET were not degraded by the chemical treating process to an extent sufficient to compromise the PAGEOS I mission.

As a result of these findings, it was decided to proceed with the full-scale treatment of the nonaluminized side of the PAGEOS I material; a solution concentration of 4.7 ppm was used. At this time, it was discovered that the results of the laboratory-scale investigation were not totally applicable to the full-scale treating machine in that a solution concentration of 4.7 ppm prevented adhesion only sporadically. The solution concentration of the full-scale treating machine was gradually increased to a point (35 ppm) where tearing due to adhesions ceased to be a problem. A 50-percent margin of safety was applied so that the solution concentration used in treating PAGEOS I material was 53 ppm. The mechanical, optical, and surface properties of the fabrication material were requalified at this level.

TABLE VI.- EFFECT OF CHEMICAL TREATMENT ON MATERIAL AND SEAM PROPERTIES

[M.D. denotes machine direction; T.D. denotes transverse roll direction]

| Test   | Detergent concentration: 4.7 and 9.4 ppm              |  |                                      | Detergent concentration: 53 ppm                      |  |                                      |
|--|---|--|--------------------------------------|--|--|--------------------------------------|
|  | Mean value $\pm$ one standard deviation               |  | Percent difference in mean value (*) | Mean value $\pm$ one standard deviation              |  | Percent difference in mean value (*) |
|  | Untreated   | Treated  |                                      | Untreated  | Treated  |                                      |
| Reflectance, percent   | 89.2 $\pm$ 0.39                                       | 89.0 $\pm$ 0.48                                      | -0.22                                | 88.7 $\pm$ 0.23                                      | 88.8 $\pm$ 0.28                                      | +0.11                                |
| Specularity, percent   | 97.1 $\pm$ 0.58                                       | 96.9 $\pm$ 0.39                                      | -0.21                                | 96.3 $\pm$ 0.35                                      | 96.2 $\pm$ 0.35                                      | -0.10                                |
| Resistivity, ohms/in <sup>2</sup>  | 0.59 $\pm$ 0.01                                       | 0.60 $\pm$ 0.08                                      | -1.7                                 | 0.67 $\pm$ 0.11                                      | 0.53 $\pm$ 0.24                                      | +20.8                                |
| Ultimate tensile strength, M.D., lb/in <sup>2</sup> (N/m <sup>2</sup> )                    | 25 900 $\pm$ 4700<br>(17.9 $\pm$ 3.2 $\times 10^7$ )  | 24 100 $\pm$ 4100<br>(16.6 $\pm$ 2.8 $\times 10^7$ ) | -6.9                                 | 26 400 $\pm$ 1700<br>(18.2 $\pm$ 1.2 $\times 10^7$ ) | 26 200 $\pm$ 2000<br>(18.1 $\pm$ 1.4 $\times 10^7$ ) | -0.76                                |
| Ultimate tensile strength, T.D., lb/in <sup>2</sup> (N/m <sup>2</sup> )                    | 31 000 $\pm$ 3100<br>(21.3 $\pm$ 2.1 $\times 10^7$ )  | 30 300 $\pm$ 3900<br>(20.9 $\pm$ 2.7 $\times 10^7$ ) | -2.3                                 | 30 500 $\pm$ 2800<br>(21.0 $\pm$ 1.9 $\times 10^7$ ) | 31 000 $\pm$ 1500<br>(21.4 $\pm$ 1.0 $\times 10^7$ ) | +1.6                                 |
| Tensile impact strength, M.D., in-lb/in <sup>3</sup> (N/m <sup>2</sup> )                   | 10 300 $\pm$ 3200<br>(7.10 $\pm$ 2.21 $\times 10^7$ ) | 9520 $\pm$ 3040<br>(6.56 $\pm$ 2.10 $\times 10^7$ )  | -7.8                                 | 7680 $\pm$ 2160<br>(5.30 $\pm$ 1.49 $\times 10^7$ )  | 6560 $\pm$ 1680<br>(4.52 $\pm$ 1.16 $\times 10^7$ )  | -14.6                                |
| Tensile impact strength, T. D., in-lb/in <sup>3</sup> (N/m <sup>2</sup> )                  | 7840 $\pm$ 3520<br>(5.41 $\pm$ 2.43 $\times 10^7$ )   | 6320 $\pm$ 2240<br>(4.36 $\pm$ 1.54 $\times 10^7$ )  | -19.4                                | 5120 $\pm$ 960<br>(3.53 $\pm$ 0.662 $\times 10^7$ )  | 5280 $\pm$ 1520<br>(3.64 $\pm$ 1.05 $\times 10^7$ )  | +3.1                                 |
| Seam ultimate tensile strength after flexure, lb/in <sup>2</sup> (N/m <sup>2</sup> )       | 28 500 $\pm$ 3100<br>(19.7 $\pm$ 2.1 $\times 10^7$ )  | 28 700 $\pm$ 3500<br>(19.8 $\pm$ 2.4 $\times 10^7$ ) | +0.70                                | 26 800 $\pm$ 1500<br>(18.5 $\pm$ 1.0 $\times 10^7$ ) | 27 000 $\pm$ 1700<br>(18.6 $\pm$ 1.2 $\times 10^7$ ) | +0.75                                |
| Seam ultimate tensile strength after thermal shock, lb/in <sup>2</sup> (N/m <sup>2</sup> ) | 28 000 $\pm$ 2500<br>(19.3 $\pm$ 1.7 $\times 10^7$ )  | 29 100 $\pm$ 3000<br>(20.1 $\pm$ 2.1 $\times 10^7$ ) | +1.0                                 | 26 100 $\pm$ 2500<br>(18.0 $\pm$ 1.7 $\times 10^7$ ) | 26 300 $\pm$ 3100<br>(18.1 $\pm$ 2.1 $\times 10^7$ ) | -0.38                                |
| Seam creep, inch (mm)  | 0.007 $\pm$ 0.003<br>(0.2 $\pm$ 0.08)                 | 0.009 $\pm$ 0.005<br>(0.2 $\pm$ 0.1)                 | -28.6                                | 0.005 $\pm$ 0.003<br>(0.1 $\pm$ 0.08)                | 0.005 $\pm$ 0.003<br>(0.1 $\pm$ 0.08)                | 0.00                                 |
| Seam peel, lb/inch of width (N/mm)   | 1.6 $\pm$ 0.2<br>(0.28 $\pm$ 0.04)                    | 1.5 $\pm$ 0.2<br>(0.26 $\pm$ 0.04)                   | -6.3                                 | 2.1 $\pm$ 0.2<br>(0.37 $\pm$ 0.04)                   | 2.0 $\pm$ 0.3<br>(0.35 $\pm$ 0.05)                   | -4.8                                 |

\* Sign indicates change in direction of improvement (+) or degradation (-).

A partial summary of the result obtained during the chemical treatment study is given in table VI. In addition, the following tests were conducted and the results were indicated:

(1) Samples of treated and untreated PAGEOS I material which were exposed to a pressure of 1 torr ( $1.33 \times 10^2$  N/m<sup>2</sup>) and a temperature of 66° C for 72 hours suffered a negligible maximum weight loss of 3 milligrams per square foot (32.3 mg/m<sup>2</sup>).

(2) Canister-simulation adhesion testing of treated samples resulted in a maximum peel force of 2.5 grams per inch of width (0.984 g/cm).

(3) Sealing-wheel adhesion testing of treated samples resulted in a maximum peel force of 3 grams per inch of width (1.18 g/cm).

(4) Exposure of the aluminized surface of the PAGEOS I material to vacuum-ultraviolet conditions ( $10^{-7}$  torr ( $0.1333 \mu\text{N/m}^2$ ), 5 "suns") for 30 days revealed no difference in solar absorptance between treated and untreated samples.

(5) Total hemispherical emittance test conducted over a temperature range of  $-25^{\circ}$  to  $120^{\circ}$  C on the PET side of the PAGEOS material showed a 7-percent decrease in the emittance of treated samples as compared with untreated samples; similar tests run on the aluminized side showed an increase of 15 percent in the emittance of the treated samples over that of the untreated samples.

Since it appeared that chemical treatment did not degrade the fabrication material to an extent which would in any way compromise the PAGEOS I mission, the process was approved for use in the remaining spheres. Later tests conducted on the interaction of the freon-detergent solution with the methylene chloride used in wiping excess adhesive from seals and on the effect of aging on the mechanical and surface properties of treated material confirmed that the chemical treatment process was satisfactory.

#### Gore-Cutting Table Shrinkage

A drop in the relative humidity in the PAGEOS area of the inflatable sphere contractor's plant from a controlled maximum level of 50 percent to 20 percent during the dry winter month of December 1965 caused a shrinkage of 0.7 inch (17.8 mm) in the 160-foot-long (48.77 m) gore-cutting table. This shrinkage caused shearing of the bolts holding the metal gore-cutting template to the tabletop to the extent that all cutting rail tolerances were exceeded. In order to stabilize the dimensions of the table so that the template could be reset, seven coats of varnish were applied to the tabletop and six to the underside of the table and its structural supports. During the course of these excursions in relative humidity, the temperature of the PAGEOS area was held at  $23^{\circ} \pm 2.7^{\circ}$  C.

The effectiveness of the varnish in dimensionally stabilizing the wooden tabletop was estimated prior to its application. By using the equilibrium moisture content of wood products and the water vapor transmission rate of the varnish, it was conservatively determined that a minimum of 180 days would be required for the tabletop dimensions to change beyond tolerances. This estimate proved to be correct since in the remaining 6 months of gore cutting, it was unnecessary to reset the template guide rails.

The varnishing of the table for dimensional stabilization was a "quick fix" designed to meet the launch schedule. In future applications, other remedies could be considered. Some of these are: (1) support of the template independent of the table, (2) use of a table material that is dimensionally stable, and (3) closer humidity control of the gore-cutting environment.

#### Canister Liner Outgassing

In order to minimize the abrasion of the inflatable spheres, the inner surface of all canisters were sprayed with a 2- to 7-mil-thick (0.051 to 0.178 mm) polymeric coating having a low coefficient of friction. During qualification and flight acceptance thermal

tests of the spacecraft, a rise in internal pressure occurred which was attributed to outgassing of the polymeric coating. As an example, the results obtained during the flight acceptance thermal test of the flight spacecraft are given in table VII. This table indicates a pressure rise of approximately 0.45 torr (60.0 N/m<sup>2</sup>) during the 120° F (48.8° C), 72-minute soak period, followed by a decrease of approximately 0.35 torr (46.7 N/m<sup>2</sup>) after completion of the test. The posttest pressure did not, however, return to the original pretest pressure. In order to confirm that outgassing and subsequent condensation of the canister liner material was responsible for the pressure behavior indicated in table VII, three samples of the coating (applied to brass shim stock) were tested under conditions simulating the flight acceptance test. The results of a typical test are shown in figure 21, where the weight change of the sample in milligrams per square foot is plotted against time. Since the thickness of the coating on both the test sample and on the canister inner surface is known only approximately, no quantitative evaluation could be made. However, figure 21 does show qualitatively that outgassing behavior of the test sample follows the same trends as the internal pressure of the canister, as reflected in table VII.

TABLE VII.- INTERNAL PRESSURE CHANGES MEASURED DURING  
FLIGHT ACCEPTANCE TEST

| Condition                    | Temperatures, °C |      |      |      | Pressures, N/m <sup>2</sup> |     |     |
|------------------------------|------------------|------|------|------|-----------------------------|-----|-----|
|                              | 1                | 2    | 3    | 4    | 1                           | 2   | 3   |
| Pretest ambient              | 26.7             | 26.7 | 26.7 | 28.1 | 67                          | 69  | 69  |
| End 72-minute soak at 120° F | 49.4             | 49.4 | 49.2 | 30.6 | 136                         | 129 | 116 |
| Posttest ambient             | 26.4             | 26.1 | 26.1 | 26.4 | 88                          | 84  | 83  |

Since an increase in spacecraft internal pressure during ascent into orbit could have caused a too rapid inflation which may have resulted in a catastrophic failure of the satellite, the acceptable spacecraft lift-off pressure was changed from 0.8 to 1.0 torr (106.6 to 133.3 N/m<sup>2</sup>) to 0.7 to 0.9 torr (93.3 to 120.0 N/m<sup>2</sup>). Actual spacecraft pressure at launch was 0.84 torr (112.0 N/m<sup>2</sup>).

#### PREFLIGHT CALCULATIONS

The PAGEOS I environment required that analyses be performed to insure that the satellite could withstand, for a period of 5 years or more, the thermal, mechanical, inflation, and radiation forces imposed upon it.



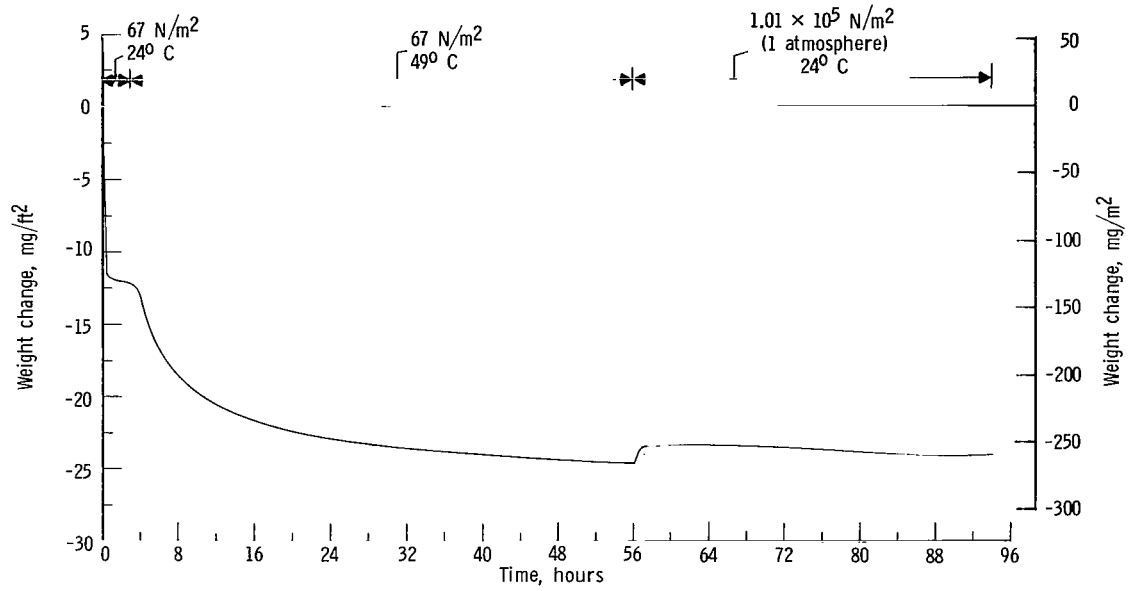


Figure 21.- Weight change as a function of time under various conditions of temperature and pressure for the PAGEOS canister liner material.

### Thermal Analysis

The following equations (derived in ref. 2) were used to calculate the average equilibrium temperature of PAGEOS I in sunlight, and the temperature of the coldest and hottest spots on its skin while in sunlight:

$$\bar{T}_{su} = \left( \frac{C_S \alpha_S}{4 \epsilon_0 \sigma} \left\{ 1 + 2 \left[ a F_R(\beta) + \frac{1-a}{4} \frac{\epsilon_0}{\alpha_S} \right] \left[ 1 - (1-k^2)^{1/2} \right] \right\} \right)^{1/4} \quad (1)$$

$$T_{C,su} = \left( \frac{1}{1 + \frac{\epsilon_0}{\epsilon_i}} \right)^{1/4} \bar{T}_{su} \quad (2)$$

$$T_{H,su} = \left[ \frac{\alpha_S}{\epsilon_i + \epsilon_0} \frac{C_S}{\sigma} + \frac{1}{1 + \frac{\epsilon_0}{\epsilon_i}} (\bar{T}_{su})^4 \right]^{1/4} \quad (3)$$

The average equilibrium temperature is of interest as a means of determining the median temperature of the satellite in a sunlit orbit for use in internal pressure and mass flow calculations. The coldspot temperature must be considered as the operating temperature when determining vapor pressure produced by the subliming compounds used for inflation. The hotspot temperature is required in evaluating the adhesive used for sealing the satellite's gores together. Other calculations were made for possible future use in the evaluation of the satellite's orbital behavior and overall performance characteristics.

Both maximum and minimum temperatures were calculated for sunlight conditions. The temperatures are a maximum when the satellite lies on the earth-sun line (that is, when  $(F_R(\beta))$  is equal to unity), and are a minimum when the satellite is about to enter the earth's shadow ( $F_R(\beta) = 0$ ). The results, an altitude of 2295 nautical miles (4250 kilometers),  $\epsilon_0 = 0.03$ ,  $\epsilon_i = 0.45$ , and  $\alpha_S = 0.10$  being assumed, are shown in table VIII. It was assumed in these and all forthcoming temperature calculations that the earth-sun line lies in the plane of the satellite orbit and that the satellite does not

TABLE VIII.- PAGEOS I TEMPERATURES IN SUNLIGHT

| Temperature    | Maximum, °C | Minimum, °C |
|----------------|-------------|-------------|
| $T_{H,su}$     | 138         | 127         |
| $\bar{T}_{su}$ | 119         | 107         |
| $T_{C,su}$     | 113         | 101         |

rotate about its own axis. These assumptions yield the most severe thermal excursions, since they place the satellite in shadow for the maximum amount of time, and also subject the satellite to the maximum temperature in sunlight, a condition that results when the satellite passes directly between the earth and the sun. The median temperature of PAGEOS I in a 2295-nautical-mile (4250-kilometer), sunlit, circular orbit was found to be 109° C.

By using the appropriate equations,  $T_{H,su}$  was calculated for the seam areas of PAGEOS I,  $\epsilon_i = 0.03$  being used for aluminum. The result, no conduction between aluminum and PET being assumed, was  $T_{H,su} = 206^\circ \text{C}$  at an altitude of 2295 nautical miles (4250 kilometers). When conduction effects were considered,  $T_{H,su}$  was found to be equal to 196° C.

The equilibrium temperature of the satellite in shadow was calculated, by use of equation (4) below, to be -132° C for an altitude of 2295 nautical miles (4250 kilometers).

$$\bar{T}_{sh} = \left\{ \frac{C_S \alpha_E}{4\epsilon_0 \sigma} \frac{1-a}{2} \left[ 1 - (1-k^2)^{1/2} \right] \right\}^{1/4} \quad (4)$$

By using equations (1) and (4),  $\bar{T}_{su}$  and  $\bar{T}_{sh}$  were also calculated as a function of altitude for various circular orbits. For each altitude selected, a maximum and minimum  $\bar{T}_{su}$  were calculated. The results are shown in table IX.

TABLE IX.- SUNLIGHT AND SHADOW TEMPERATURES  
AS A FUNCTION OF ALTITUDE

| Altitude   |                | $\bar{T}_{su}, ^\circ\text{C}$ |         | $\bar{T}_{sh}, ^\circ\text{C}$ |
|------------|----------------|--------------------------------|---------|--------------------------------|
| Kilometers | Nautical miles | Maximum                        | Minimum |                                |
| 2000       | 1080           | 129                            | 108     | -97                            |
| 4000       | 2160           | 120                            | 107     | -122                           |
| 4250       | 2295           | 119                            | 106     | -130                           |
| 5000       | 2700           | 117                            | 106     | -134                           |
| 6600       | 3564           | 114                            | 106     | -147                           |

The times necessary for PAGEOS I to reach an equilibrium temperature in its passage from sunlight to shadow  $t_{sh}$  and from shadow to sunlight  $t_{su}$  were calculated by use of the following equations which are derived in appendix A of reference 2:

$$t_{sh} = \frac{y^2}{2\omega x \sqrt{\omega/x}} \left( \tan^{-1} \frac{\bar{T}}{\sqrt{\omega/x}} - \frac{1}{2} \log_e \frac{\bar{T} - \sqrt{\omega/x}}{\bar{T} + \sqrt{\omega/x}} \right) - \frac{z^2}{4\omega x} \left( \log \frac{\bar{T}^2 - \omega/x}{\bar{T}^2 + \omega/x} \right) \frac{\bar{T}}{\bar{T}_0} \quad (5)$$

$$t_{su} = \frac{y^2}{2\omega_1 x \sqrt{\omega_1/x}} \left( \tan^{-1} \frac{\bar{T}}{\sqrt{\omega_1/x}} + \frac{1}{2} \log_e \frac{\sqrt{\omega_1/x} + \bar{T}}{\sqrt{\omega_1/x} - \bar{T}} \right) + \frac{z^2}{4\omega_1 x} \left( \log_e \frac{\omega_1/x + \bar{T}^2}{\omega_1/x - \bar{T}^2} \right) \Bigg|_{\bar{T}_0}^{\bar{T}} \quad (6)$$

where

$$x^2 = \frac{\pi D^2 \epsilon_o \sigma}{m}$$

$$\omega^2 = \frac{\pi D^2 C_S \alpha_E K}{4m} \left( \frac{1-a}{2} \right)$$

$$\omega_1^2 = \frac{\pi D^2 C_S \alpha_S K}{4m} \left[ 1 + \left( 2a F_R(\beta) + \frac{\alpha_E}{\alpha_S} \frac{1-a}{2} \right) \right]$$

$$K = 1 - (1 - k^2)^{1/2}$$

and  $y$  and  $z$  are specific constants used to define the specific heat. The results (fig. 22) indicate that  $t_{sh} = 38$  minutes and  $t_{su} = 8$  minutes.

#### Deforming Loads

By the use of equations (7) and (8) which follow (from ref. 2), the deforming loads on the passive geodetic satellite and the critical buckling pressure of its skin were

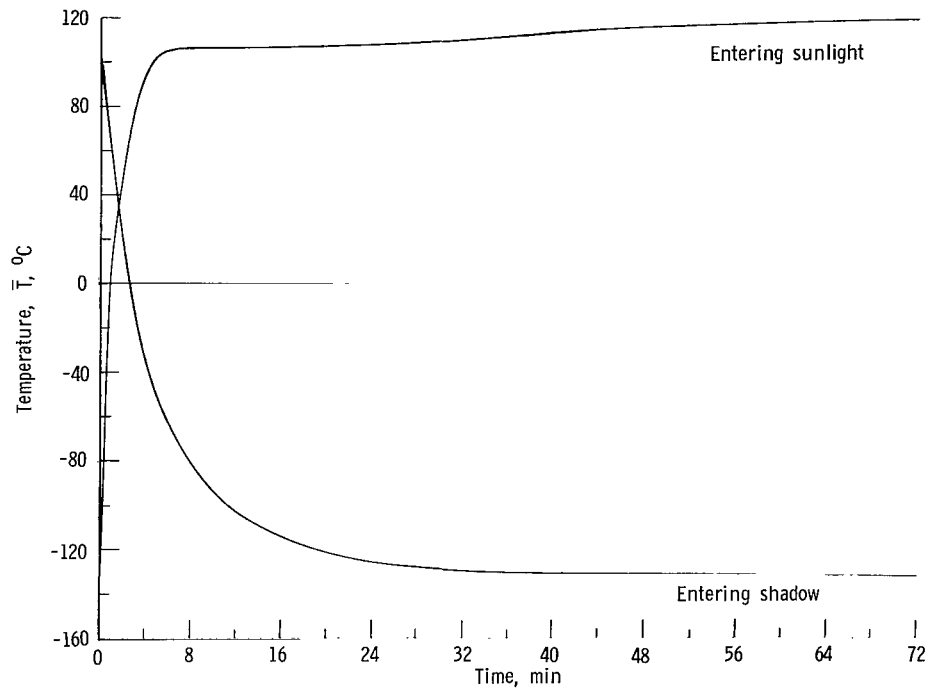


Figure 22.- Dynamic thermal response of PAGEOS in its passage from sunlight to shadow and shadow to sunlight.

calculated. Since the minimum perigee of the satellite for its 5-year lifetime is predicted to be 1080 nautical miles (2000 kilometers), only the solar radiation pressure was found to be a significant deforming load. This pressure, which is independent of altitude in near-earth orbits, was calculated from the equation

$$p_s = \frac{2C_s}{c} = 6.98 \times 10^{-8} \text{ torr } (9.30 \times 10^{-6} \text{ N/m}^2) \quad (7)$$

The critical buckling pressure of a smooth, thin-walled sphere is given by

$$p_{cr} = \frac{2E(t')^2}{R_b^2 [3(1 - \nu^2)]^{1/2}} = 2.68 \times 10^{-5} \text{ torr } (3.57 \times 10^{-3} \text{ N/m}^2) \quad (8)$$

The ratio  $p_{cr}/p_s$ , which is the deformation safety factor, was calculated, by use of equations (7) and (8), to be 384.

#### Internal Pressure and Mass Flow

In the interest of orbital perturbation and precession calculations, the mass flow rate of the PAGEOS I inflation compounds out of the satellite was calculated as a function of time by use of the equation (from ref. 2)

$$-\frac{dm}{dt} = \left(\frac{1}{2\pi R_g}\right)^{1/2} \left[ p_b \left(\frac{M_b}{T}\right)^{1/2} + p_a \left(\frac{M_a}{T}\right)^{1/2} \right] (f + gt) \quad (9)$$

The numerical value used for  $g$  in this and following equations is believed to be an upper limit.

At the time of full inflation, the benzoic acid is completely vaporized and exerts a pressure given by

$$p_{o,b} = \frac{W_b R_g T}{M_b V} \quad (10)$$

This initial pressure decreases from its original value due to leakage through air orifices built into the satellite structure, and through those holes caused by micrometeoroid puncture, in accordance with the following equation, which is derived in appendix B of reference 2:

$$p_b = p_{o,b} \exp \left[ -R_g \left(\frac{1}{2\pi R_g}\right)^{1/2} \left(\frac{T}{M_b V^2}\right)^{1/2} \left( ft + \frac{1}{2} gt^2 \right) \right] \quad (11)$$

The anthraquinone present in the sphere at the time of full inflation is in solid-vapor equilibrium and exerts a pressure given by

$$\log_e p_{o,a} = 40.145 - \frac{15206}{T} \quad (12)$$

The time at which all the solid anthraquinone present is vaporized and begins to act in accordance with an equation similar to equation (10) is given by

$$m_a - \frac{p_{O,a}VM_a}{R_gT} = \left(\frac{M_a}{2\pi R_gT}\right)^{1/2} \left(ft + \frac{1}{2}gt^2\right)p_{O,a} \quad (13)$$

where  $m_a$  represents the original mass of anthraquinone and the second term on the left represents the amount of the compound in the vapor state required to sustain an equilibrium pressure. Solution of equation (13) for 109° C yields  $t = 303$  hours. When all the anthraquinone is vaporized, its pressure decreases with extreme rapidity because of the micrometeoroid hole area accumulated by this time.

The contributions of both benzoic acid and anthraquinone to the internal pressure at 109° C were added together with the results shown in figure 23. At the time when full

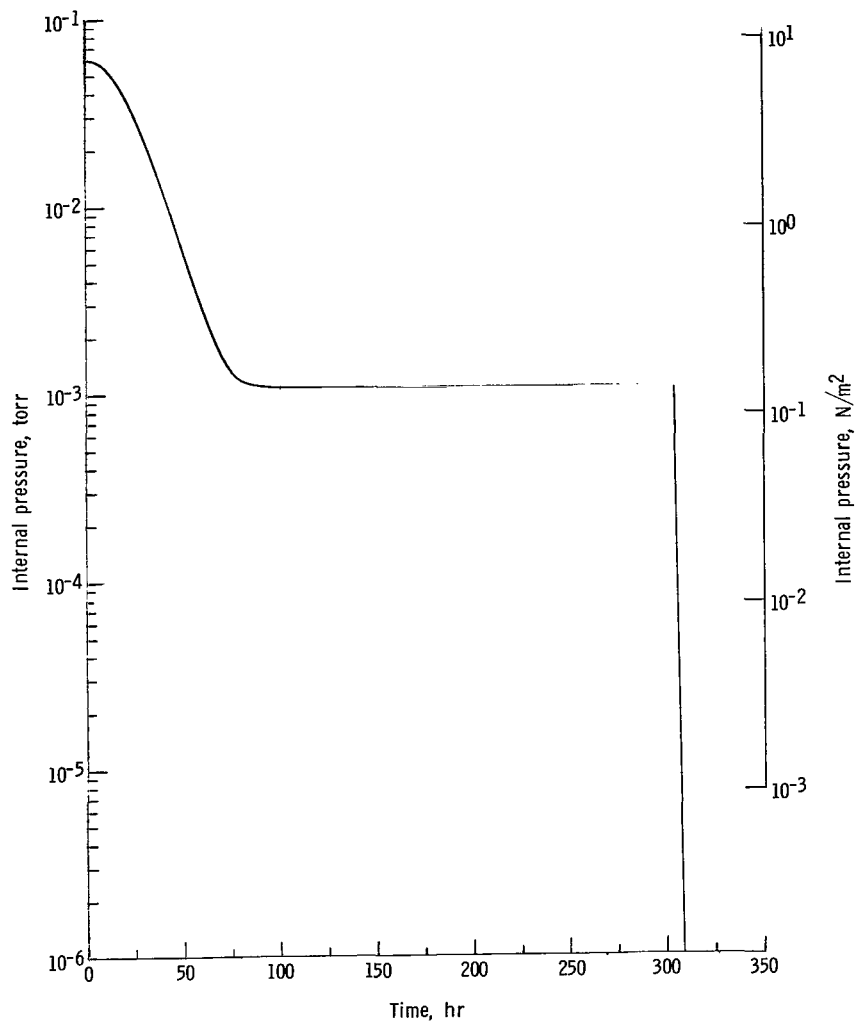


Figure 23.- Predicted internal pressure history of PAGEOS as a function of time after inflation.

inflation is completed, the major contribution to the internal pressure is made by vaporized benzoic acid. At the same time, the anthraquinone is in solid-vapor equilibrium and maintains a steady, but lower, pressure. The benzoic acid vapor escapes rapidly through the holes in the satellite's skin (and thus causes an initial steep decrease in internal pressure) until a point is reached at which its contribution, relative to that of anthraquinone, becomes negligible. The anthraquinone maintains its steady pressure contribution until it is all vaporized, at which time the pressure drops off sharply again.

The combined mass flow rate of benzoic acid and anthraquinone is plotted in figure 24 as a function of time for a temperature of 109° C. The initial rapid increase in

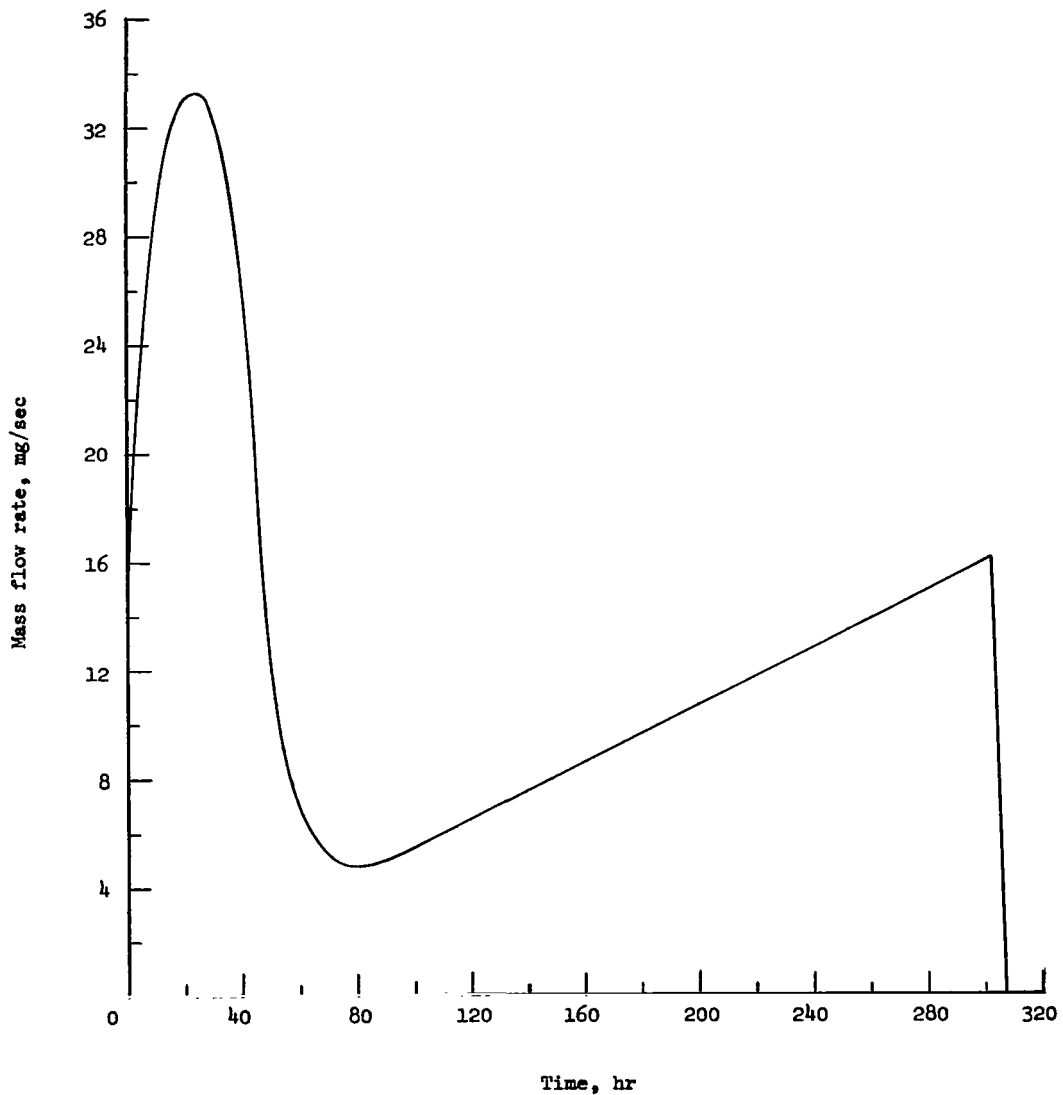


Figure 24.- Predicted mass flow rate of the inflation compounds, benzoic acid and anthraquinone, from PAGEOS while in a continuous sunlight orbit.

mass flow rate is due to the initial high vapor pressure of benzoic acid and the increase in micrometeoroid hole area. At about 25 hours, the mass flow rate decreases rapidly because the micrometeoroid holes have accumulated to such size that the rate of partial pressure decrease has become the controlling parameter rather than hole growth rate. Between 85 and 90 hours the slope changes sharply again; this change reflects depletion of the benzoic acid and predominance of the anthraquinone vapor flow. The vapor pressure of anthraquinone remains constant until all the solid is gone and its increasing rate of flow is governed entirely by the increase in micrometeoroid hole area. When the supply of solid anthraquinone is depleted, the flow rate decreases rapidly because of a lack of constant pressure.

By integrating equation (9), the satellite mass as a function of time after deployment was calculated. The results are shown in figure 25. An initial balloon mass (including contents) of 149.8 pounds (68.0 kg) and an inflation powder mass of 30.6 pounds (13.9 kg) were used. It was assumed that the satellite and its contents were at a temperature of 109° C.

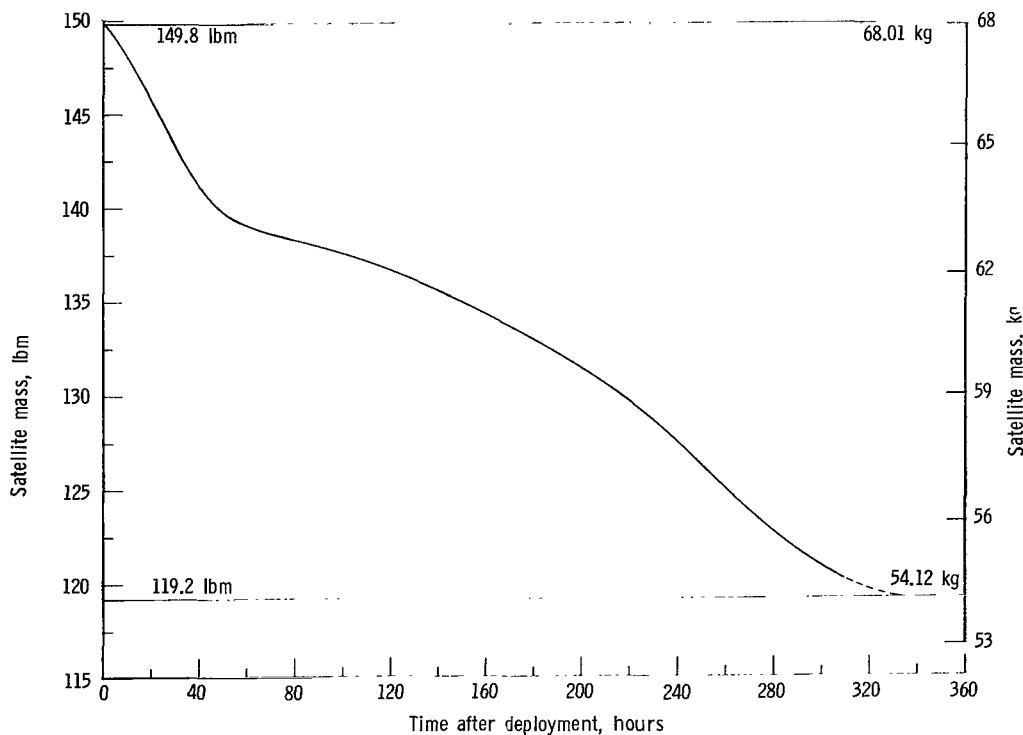


Figure 25.- Predicted PAGEOS I mass as a function of time after deployment.



## Inflation Mechanics Study

To start its 5-year mission successfully, the PAGEOS I satellite had to inflate to its full size without tearing. In order to achieve this objective, a number of requirements were established:

(1) Use of an erectable fabrication material which could withstand the loads imposed upon it by the inflation process

(2) Use of a folding pattern which would satisfy the requirements of compactness and simultaneously minimize stress concentrations

(3) Use of benzoic acid and anthraquinone, which sublimed under the impetus of solar heating, with control of the generated pressure by the amount of the inflatants used, as done successfully in Echo I

(4) The canister be designed to maintain an internal pressure of 0.7 to 0.9 torr (93.3 to 120.0 N/m<sup>2</sup>) for long periods; a passive thermal control pattern be employed to maintain a temperature of 0° to 60° C during balloon confinement

(5) Selection of a continuous sunlight orbit of 14 or more days in duration to insure the sustenance of a positive skin stress sufficient to prevent collapse under solar pressure or fold memory until such time as the skin stresses produced by folding were relaxed.

The design criteria employed to satisfy these conditions were largely based on prior Echo I technology. However, as a means of confirming some of the empirical data used in establishing these criteria, a theoretical study of the inflation mechanics of Echo-type inflatable spheres was initiated.

A two-stage mathematical model (ref. 11) was developed to predict inflation times, skin stresses, and skin velocities. In this model, the first stage accounts for the deployment of the accordion folds and the second stage accounts for the unfolding of the pleat folds. The transition stage, during which both the accordion folds and the pleat folds are being opened, is not considered because of the current lack of an adequate mathematical model to represent it. Instead, the two stages employed are considered sequentially. At the end of the second stage, an additional stress analysis is carried out.

The significant parameters in the solution of the mathematical model are: (1) the fabrication material properties such as thickness, modulus, and Poisson's ratio, (2) the folding configuration, as exemplified by the number and height of the accordion and pleat folds, (3) the full size and weight of the inflatable sphere, and (4) the internal pressure. The actual solution for velocity, stress, and inflation time is accomplished numerically by a high-speed computer.

If the initial internal residual air pressure is varied from 0.5 to 1.5 torr (66.7 to 200 N/m<sup>2</sup>) and the internal temperature from 32° to 150° F (0° to 65.6° C), by using benzoic acid and anthraquinone inflatants, the maximum skin velocity was predicted to range from 15 to 43 feet per second (4.57 to 13.11 m/sec) during inflation. Under these same conditions, the maximum skin stress was predicted to vary from 837 to 2591 psi (5.77 to 17.9 MN/m<sup>2</sup>).

For conditions similar to those of the deployment test, the mathematical model predicts a velocity of 18 feet per second (5.48 m/sec) for the first stage, and is in excellent agreement with experimental results. For conditions similar to those to which PAGEOS I was exposed in its canister immediately prior to inflation, the mathematical model predicts an inflation time of approximately 13 seconds while photographic observations of the actual inflation indicate an inflation time of 16 seconds.

#### Electron Radiation Effects

PAGEOS I will spend a large percentage of its orbital lifetime in the inner Van Allen belt – a region of high intensity, magnetically trapped, particulate radiation which extends from 1080 to 2592 nautical miles (2000 to 4800 kilometers) above the earth. In order to fulfill the mission requirements, the structural integrity of the satellite's load-bearing PET film and the reflectance of its vapor-deposited aluminum surface must be maintained for 5 years. It was therefore necessary to estimate the radiation doses to which the aluminized PET film of the inflatable satellite would be subjected in orbit. Since the contribution of high-energy protons, such as those found in the inner Van Allen belt, to the radiation dose absorbed by thin films is negligible, the calculations were limited to electron effects.

Reference 12 describes a numerical method for determining the amount of energy deposited in thin films of low atomic number by single, normally incident electrons with energies up to 5 MeV ( $8.0 \times 10^{-13}$  joule). An expression is derived which permits the calculation of the average path length, as a function of incident energy, of an electron penetrating a material for which the atomic density, atomic number, and mean excitation potential are known. A procedure is then presented for determining the amount of energy deposited in a given material of known thickness by individual electrons of a particular incident energy by use of the aforementioned expression. The expressions derived in reference 12 are based on the assumption that the material absorbs all the energy deposited by the incident particles. This assumption is valid since the predominant mode of energy loss is through the processes of ionization and excitation and little energy, if any, is lost by radiation (Bremsstrahlung). Table X gives the results obtained for energy absorbed by the aluminum and PET layers of PAGEOS I due to electrons of various energies. This table shows that peak absorption occurs at an incident electron energy of

4 keV ( $6.4 \times 10^{-16}$  joule) for aluminum and 30 keV ( $4.8 \times 10^{-15}$  joule) for PET. If, in each case, a flux of  $10^7$  electrons  $\text{cm}^{-2} \text{sec}^{-1}$  (ref. 13) is assumed, the maximum dose absorbed was calculated to be 340 megarads ( $3.40 \times 10^6$  joule/kg) per year for aluminum and 42 megarads ( $4.2 \times 10^5$  joule/kg) per year for PET.

TABLE X. - ELECTRON ENERGY DEPOSITION IN ALUMINUM AND PET

| Incident electron energy |                       | Energy absorbed per electron by - |                       |      |                       |
|--------------------------|-----------------------|-----------------------------------|-----------------------|------|-----------------------|
|                          |                       | Aluminum                          |                       | PET  |                       |
| keV                      | joule                 | keV                               | joule                 | keV  | joule                 |
| 1                        | $1.6 \times 10^{-16}$ | 1                                 | $1.6 \times 10^{-16}$ | 1    | $1.6 \times 10^{-16}$ |
| 4                        | 6.4                   | 4                                 | 6.4                   | 4    | 6.4                   |
| 5                        | 8.0                   | 1.8                               | 2.8                   | 3.2  | 5.1                   |
| 10                       | $1.6 \times 10^{-15}$ | .7                                | 1.1                   | 9.3  | $1.5 \times 10^{-15}$ |
| 20                       | 3.2                   | .4                                | $6.4 \times 10^{-17}$ | 19.6 | 3.1                   |
| 30                       | 4.8                   | .3                                | 4.8                   | 29.7 | 4.8                   |
| 50                       | 8.0                   | .2                                | 3.2                   | 11.9 | 1.9                   |
| 100                      | $1.6 \times 10^{-14}$ | .1                                | 1.6                   | 7.1  | 1.1                   |
| 1500                     | $2.4 \times 10^{-13}$ | .05                               | $8.0 \times 10^{-18}$ | 3.1  | $5.0 \times 10^{-16}$ |
| 5000                     | 8.0                   | .06                               | 9.6                   | 3.6  | 5.8                   |

In addition, an estimate was made which indicates that PAGEOS I will spend 30 percent of its lifetime within the altitude (1080 to 2592 nautical miles or 2000 to 4800 kilometers) and latitude ( $70^\circ$  N to  $70^\circ$  S) boundaries assumed for the inner Van Allen belt. Thus, the resulting absorbed doses for electrons of 4 and 30 keV ( $6.4 \times 10^{-16}$  and  $4.8 \times 10^{-15}$  joule) impinging on aluminum and PET for an assumed 5-year satellite lifetime are 510 megarads ( $5.10 \times 10^6$  joule/kg) and 63 megarads ( $6.3 \times 10^5$  joule/kg), respectively.

After exposure to 70 megarads ( $7.0 \times 10^5$  joule/kg) of electron-simulating gamma radiation, PET retained 70 percent of its original ultimate tensile strength, 69 percent of its original ultimate elongation, and 50 percent of its original energy to break. Since the maximum skin stress on the satellite during its 5-year lifetime (exclusive of the short-period inflation process itself) will be 750 pounds per square inch ( $5.17 \text{ MN/m}^2$ ), a more than adequate margin of safety is present.

Additional studies indicate a decrease in reflectance of the aluminized surface of the PAGEOS I material of approximately 25 percent at an exposure level of 518 megarads ( $5.18 \text{ MJ/kg}$ ). The tests were conducted on gamma-irradiated specimens of PAGEOS I material enclosed in a sealed container from which any PET degradation products could not escape as they would in space. In these respects the test conditions were not

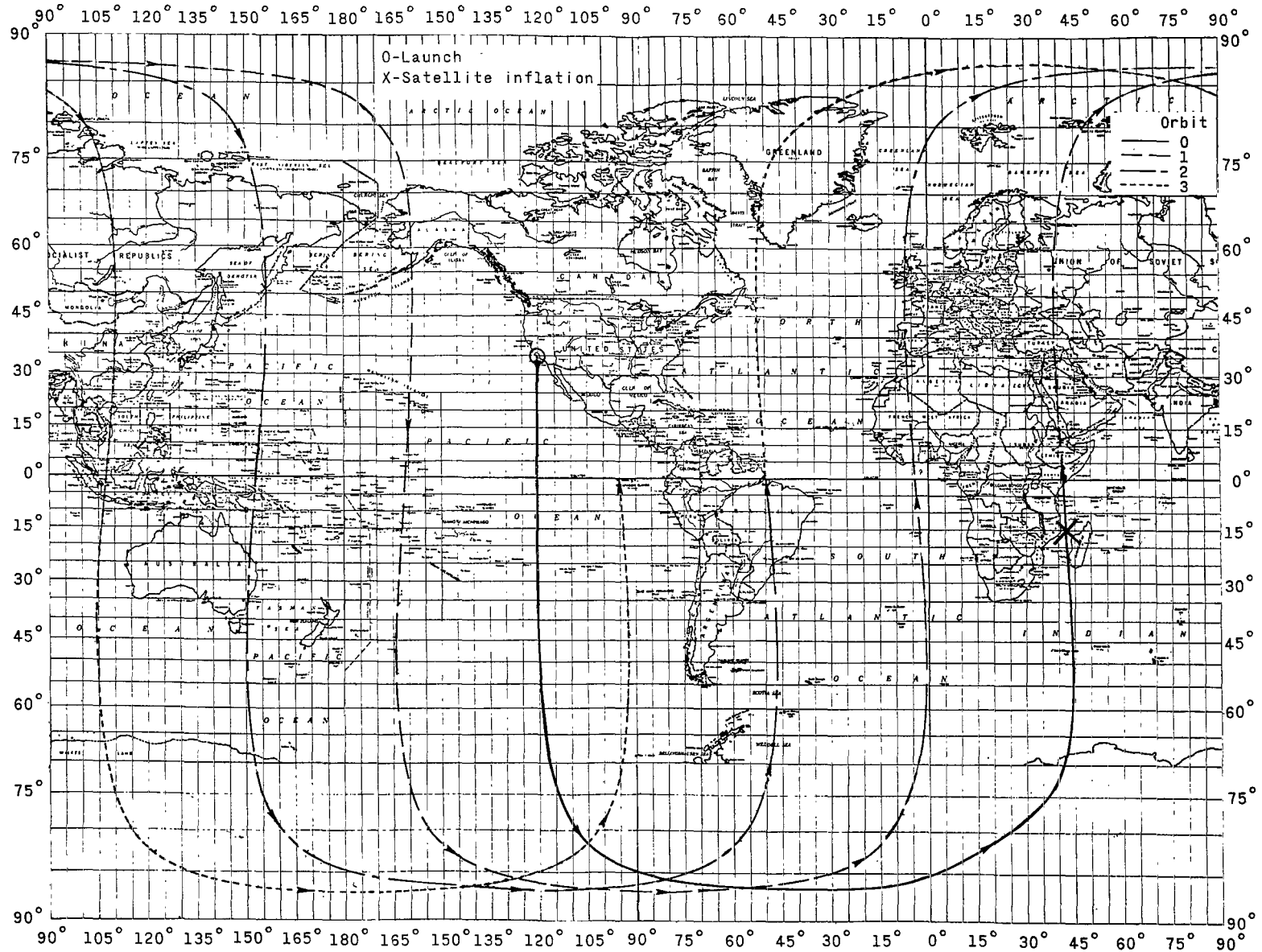


Figure 26.- Predicted suborbital plot of PAGEOS 1 for first three orbits.

comparable with those to be found in the space environment. However, even such a large decrease in reflectance as that indicated would not jeopardize the ability of PAGEOS I to perform its geodetic mission.

## PERFORMANCE CHARACTERISTICS

### Orbit Injection

Lift-off of PAGEOS I from the U.S. Air Force Western Test Range at South Vandenburg Air Force Base, California, occurred at 00:12 G.m.t. on June 24, 1966. Deployment occurred approximately 72.5 minutes later off the southeastern coast of Africa. The transfer orbit and the first three orbits after injection are shown in figure 26. The initial nominal and actual satellite orbits are compared in table XI. This table also shows the maximum variation in orbital parameters for a 5-year period predicted by the modified computer program.

TABLE XI.- INITIAL ORBITAL PARAMETERS AND THEIR  
PREDICTED MAXIMUM 5-YEAR VARIATION

| Orbital parameter              | Nominal | Actual    | Maximum variation |
|--------------------------------|---------|-----------|-------------------|
| Semimajor axis, kilometers . . | 10 628  | 10 614.79 | 10 551.26         |
| Eccentricity . . . . .         | 0.0000  | 0.000248  | 0.205792          |
| Inclination, degrees . . . . . | 87.00   | 86.9739   | 83.7605           |
| Apogee, kilometers . . . . .   | 4250    | 4262.94   | 6344.48           |
| Perigee, kilometers . . . . .  | 4250    | 4210.30   | 2001.73           |

### Photometric Observation

By use of a truck-mounted mobile observatory consisting of a 24-inch (0.610 m) telescope, photometric instrumentation capable of making brightness measurements in the three color bands of the standard ultraviolet-blue-visible photometric system (ref. 14), and associated electronic equipment, the size, shape, and surface characteristics of PAGEOS I were determined for the first 60 days of the satellite's orbital life. Raw brightness data as a function of the relative positions of the sun, the satellite, and the observer were obtained at Palomar Mountain, California, for later reduction to PAGEOS I stellar magnitude, solar reflectance and specularity, and radius of curvature. The results of these observations are summarized in table XII, where the data are divided into preshadow and postshadow periods. The data are divided into these two periods because, coincident with the satellite's first entrance into shadow on July 16, 1966 and the predicted simultaneous loss of anthraquinone sustaining pressure, PAGEOS I began

TABLE XII.- RESULTS OF PHOTOMETRIC OBSERVATIONS

| Parameter                                  | Visible band   |                            |                            | Blue band      |                            |                            | Ultraviolet band |                            |                            |
|--|----------------|----------------------------|----------------------------|----------------|----------------------------|----------------------------|------------------|----------------------------|----------------------------|
|  | Nominal        | Preshadow                  | Postshadow                 | Nominal        | Preshadow                  | Postshadow                 | Nominal          | Preshadow                  | Postshadow                 |
| Stellar magnitude                          | 2.23           | 2.18 ± 0.21                | 2.14 ± 0.27                | 2.87           | 2.84 ± 0.22                | 2.79 ± 0.28                | 2.94             | 3.00 ± 0.21                | 2.95 ± 0.28                |
| Reflectance, percent                       | 89.6           | 87.0                       | 89.0                       | 89.6           | 85.4                       | 86.3                       | 88.4             | 77.9                       | 78.9                       |
| Specular component of reflectance, percent | 96.9           | 98.5                       | 98.9                       | 96.9           | 99.3                       | 95.9                       | 96.9             | 103.4                      | 96.2                       |
| Average radius of curvature, feet (m)      | 50.0<br>(15.2) | 49.5 ± 5.1<br>(15.1 ± 1.5) | 50.2 ± 6.5<br>(15.3 ± 2.0) | 50.0<br>(15.2) | 49.1 ± 4.9<br>(15.0 ± 1.5) | 49.5 ± 7.1<br>(15.1 ± 2.2) | 50.0<br>(15.2)   | 47.2 ± 4.6<br>(14.4 ± 1.4) | 47.6 ± 6.5<br>(14.5 ± 2.0) |

to exhibit scintillations of brightness. This behavior is evidenced by an increase in the standard deviation of the average radius of curvature. The results presented in table XII indicate that, on the average, the satellite's brightness, size, and shape are extremely close to the design values.

A detailed account of the theory, instrumentation, and calibration and reduction procedures employed in obtaining these results is given in reference 15.

#### CONCLUDING REMARKS

The fabrication and testing of PAGEOS I and the attendant accumulation of a large body of data on process techniques and materials behavior has significantly advanced the state of the art of inflatable sphere technology. The engineering program which this fabrication and testing represent was culminated with the successful launch and deployment of PAGEOS I.

Langley Research Center,  
 National Aeronautics and Space Administration,  
 Langley Station, Hampton, Va., November 27, 1967,  
 855-00-00-00-23.

## REFERENCES

1. Rosenberg, Jerome D.: The Organization of the United States Geodetic Satellite Program. Paper presented at the Symposium for the Establishment of a European Geodetic Network Using Artificial Satellites (Paris, France), Dec. 1964.
2. Clemmons, Dewey L., Jr.: The Echo I Inflation System. NASA TN D-2194, 1964.
3. Anon.: Satellite Triangulation in the Coast and Geodetic Survey. Tech. Bull. No. 24, Coast and Geodetic Survey, U.S. Dept. Commerce, Feb. 1965.
4. Dufour, H. M.: Geodetic Junction of France and North Africa by Synchronized Photographs Taken From the Echo I Satellite. NASA TT F-9388, 1965.
5. Shchegolov, D. E.; Masevich, A. G.; and Afanas'yev, B. G.: Simultaneous Tracking of the Balloon Satellite Echo I for Geodetic Purposes. ST-SSA-10201 (Contract NAS-5-3760), Goddard Space Flight Center, Sept. 4, 1964.
6. Anon.: Photometric Measurements of Surface Characteristics of Echo I Satellite – Final Report. GER 11648 (Contract NAS1-3114, Amendment 5), Goodyear Aerospace Corp. June 19, 1964.
7. Worley, S.; Miller, J.; and Linsenmayer, G.: Orbit Selection Study for PAGEOS Satellite. Final Rept. (Contract NAS1-4614), Westinghouse Electric Corp., May 1965.
8. Bowker, David E.: PAGEOS Project – Compilation of Information for Use of Experimenter. NASA TM X-1344, 1967.
9. Gibson, James O.; and Carman, Robert R.: Passive Geodetic Satellite Canister Assemblies. NASA CR-700, 1967.
10. Stenland, S. J.; Dahlgren, C. A.; Wendt, A. J.; Lingo, D.; Roiseland, D.; and Neuhaus, T. J.: Passive Geodetic Satellite Inflatable Sphere Assemblies. NASA CR-66,274, G. T. Schjeldahl Co., [Dec. 1966].
11. Saleme, Ernesto: Passive Geodetic Satellite Inflation Rate Study. NASA CR-746, 1967.
12. Teichman, Louis A.; and Armstrong, Ernest S.: Calculation of Electron Energy Deposition in Thin-Film Polymeric Materials. NASA TN D-2010, 1963.
13. Hess, Wilmot N.: Energetic Particles in the Inner Van Allen Belt. NASA TN D-1749, 1963.

14. Johnson, H. L.: Photometric Systems. Basic Astronomical Data, K. A. Strand, ed., Univ. Chicago Press, c.1963, pp. 204-224.
15. Hostetler, R. L.; Emmons, R. H.; Preski, R. J.; Rogers, C. L.; and Romick, D. C.: Ground-Based Photometric Surveillance of the Passive Geodetic Satellite. NASA CR-791, 1967.



FIRST CLASS MAIL

POSTMASTER: If Undeliverable (Section 158  
Postal Manual) Do Not Return

*"The aeronautical and space activities of the United States shall be conducted so as to contribute . . . to the expansion of human knowledge of phenomena in the atmosphere and space. The Administration shall provide for the widest practicable and appropriate dissemination of information concerning its activities and the results thereof."*

— NATIONAL AERONAUTICS AND SPACE ACT OF 1958

## NASA SCIENTIFIC AND TECHNICAL PUBLICATIONS

**TECHNICAL REPORTS:** Scientific and technical information considered important, complete, and a lasting contribution to existing knowledge.

**TECHNICAL NOTES:** Information less broad in scope but nevertheless of importance as a contribution to existing knowledge.

**TECHNICAL MEMORANDUMS:** Information receiving limited distribution because of preliminary data, security classification, or other reasons.

**CONTRACTOR REPORTS:** Scientific and technical information generated under a NASA contract or grant and considered an important contribution to existing knowledge.

**TECHNICAL TRANSLATIONS:** Information published in a foreign language considered to merit NASA distribution in English.

**SPECIAL PUBLICATIONS:** Information derived from or of value to NASA activities. Publications include conference proceedings, monographs, data compilations, handbooks, sourcebooks, and special bibliographies.

**TECHNOLOGY UTILIZATION PUBLICATIONS:** Information on technology used by NASA that may be of particular interest in commercial and other non-aerospace applications. Publications include Tech Briefs, Technology Utilization Reports and Notes, and Technology Surveys.

*Details on the availability of these publications may be obtained from:*

SCIENTIFIC AND TECHNICAL INFORMATION DIVISION  
NATIONAL AERONAUTICS AND SPACE ADMINISTRATION  
Washington, D.C. 20546